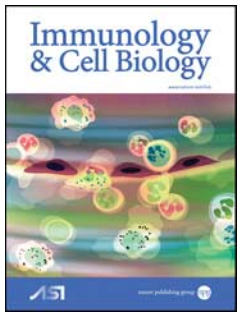

Actin polymerization-dependent activation of Cas-L promotes immunological synapse stability

Luís C Santos, David A Blair, Sudha Kumari, Michael Cammer, Thomas Iskratsch, Olivier Herbin, Konstantina Alexandropoulos, Michael L Dustin, Michael P Sheetz

Cite this article as: Luís C Santos, David A Blair, Sudha Kumari, Michael Cammer, Thomas Iskratsch, Olivier Herbin, Konstantina Alexandropoulos, Michael L Dustin, Michael P Sheetz, Actin polymerization-dependent activation of Cas-L promotes immunological synapse stability, *Immunology and Cell Biology* accepted article preview 30 June 2016; doi: 10.1038/icb.2016.61.

Received 18 January 2016; revised 6 June 2016; accepted 20 June 2016; Accepted article preview online 30 June 2016

Actin polymerization-dependent activation of Cas-L promotes immunological synapse stability

Running title: Cas-L coordinates T cell actin cytoskeleton.

Luís C. Santos,[§,†] David A. Blair,[†] Sudha Kumari,[†] Michael Cammer,[†] Thomas Iskratsch,[§] Olivier Herbin,[¶] Konstantina Alexandropoulos,[¶] Michael L. Dustin,[†, ‡,*] and Michael P. Sheetz[§,*]

[§] Department of Biological Sciences, Columbia University, New York, NY 10027 USA;

[†] Skirball Institute of Biomolecular Medicine, New York School of Medicine, New York, NY 10012 USA;

[¶] Icahn Medical Institute, Mount Sinai School of Medicine, New York, NY 10029, and

[‡] Kennedy Institute of Rheumatology, University of Oxford, Headington, OX3 7FY, UK.

[*] Corresponding authors: Michael P. Sheetz, PhD, Department of Biological Sciences, Columbia University, MB2416, 713 Fairchild Center, 1212 Amsterdam Ave., New York, NY 10027; e-mail address: ms2001@columbia.edu; contact number: +1 (212)-854-8133. Fax: +1 (212)-854-6399; or Michael L. Dustin, PhD, The University of Oxford and Kennedy Institute of Rheumatology, Roosevelt Drive, Headington, Oxford, OX3 7FY, UK; e-mail address michael.dustin@kennedy.ox.ac.uk; contact number: +44 (0)1865 612639 (direct), Fax: +44 (0)1865 612601.

This work was supported by National Institutes of Health Common Fund through a Nanomedicine Development Center PN2EY016586 (M.L.D., M.P.S.). O.H. and K.A. were

supported by N.I.H. grants R01 AI068963-01A2 and R01 AI088106-01A1. The Wellcome Trust and the Kennedy Institute of Rheumatology Trust supported M.L.D.

The authors declare no conflict of interest.

The online version of this article contains supplementary material.

Keywords: Cas-L, actin polymerization, tyrosine phosphorylation, immunological synapse, supported lipid bilayer, mechanotransduction.

Abstract

The immunological synapse formed between a T cell and an antigen presenting cell is important for cell-cell communication during T cell mediated immune responses. Immunological synapse formation begins with stimulation of the T cell receptor (TCR). TCR microclusters are assembled and transported to the center of the immunological synapse in an actin polymerization dependent process. However, the physical link between TCR and actin remains elusive. Here we show that lymphocyte-specific Crk-associated substrate (Cas-L), a member of a force sensing protein family, is required for transport of TCR microclusters and for establishing synapse stability. We found that Cas-L is phosphorylated at TCR microclusters in an actin polymerization-dependent fashion. Furthermore, Cas-L participates in a positive feedback loop leading to amplification of Ca^{2+} signaling, inside-out integrin activation, and actomyosin contraction. We propose a new role for Cas-L in T cell activation as a mechanical transducer linking TCR microclusters to the underlying actin network and coordinating multiple actin dependent structures in the immunological synapse. Our studies highlight the importance of mechanotransduction processes in T cell mediated immune responses.

Introduction

Most adaptive immune responses require activation of T cells [1-3]. The process of T cell activation involves a multi-step mechanism that begins with weak adhesion and stimulation of the T cell receptor (TCR) leading to adhesion strengthening and formation of a highly organized immunological synapse [4-7]. Spatial organization of the immunological synapse requires f-actin [8-10], myosin IIA [11-13], microtubules and dynein [14], and the endosomal sorting complexes required for transport [15, 16]. There is growing evidence supporting a physical link between TCR microclusters and the actin cytoskeleton, but this most fundamental connection is the most poorly understood [17-20]. TCR and integrin adhesion molecules organize actin polymerization [21-23] that drives transport of distinct TCR and integrin microclusters toward the center of the synapse [24-27]. This can be modeled as a "frictional" process as the bulk flow of f-actin is faster than the movement of microclusters, but the molecular basis of the friction-like effect is not known. Furthermore, the TCR and integrins have been implicated in mechanotransduction at the immunological synapse [28-31], but how the TCR participates in mechanotransduction remains unknown.

The temporal and spatial localization of signaling proteins at the immunological synapse correlates with T cell activation. Proper assembly and localization of signaling complexes is often mediated by scaffold proteins [32]. These multidomain adaptors have several binding partners, and by bringing them into close proximity they facilitate protein-protein interactions and signal propagation. Although many scaffold proteins are essential for T cell activation, how they become activated and how they regulate T cell signals is largely unknown. We recently described a model for actin-dependent stretch of the mechanosensing protein p130 Crk-associated substrate (p130Cas) [33] used by cells in sensing their physical environment, in integrin

adhesions, and during migration [34-37]. p130Cas belongs to a family of adaptor proteins that share a flexible Cas substrate domain that unfolds in response to force exposing Src family kinase phosphorylation sites [38]. The Cas family member most abundant in T cells is Cas-L (also called Hef1 and NEDD9) [39, 40]. Cas-L contains a central substrate domain with 13 repeated motifs each containing a tyrosine residue (YxxP), flanked on one side by an N-terminal SH3 domain, and on the other by a proline-rich four-helix bundle and a Src-family kinase-binding domain with consensus binding sites YDYVHL and RPLPSPP, for SH2 and SH3 domains, respectively. Although Cas-L does not have any enzymatic activity, it has been implicated in a diverse set of physiological and pathological contexts in different cell types [41-47]. This functional versatility underscores the importance of Cas-L in mediating receptor-proximal interactions and propagating local stimulatory signals that lead to global changes in cell behavior [32, 48].

Seo and colleagues [49] observed that Cas-L$^{-/-}$ mice have a decreased number of lymphocytes in peripheral lymphoid organs, a thin marginal zone, an impaired TCR-induced response to immunization with a specific peptide, and perturbed integrin-mediated adhesion in comparison to wild type mice. Previous studies reported that following TCR and integrin stimulation the Cas-L substrate domain tyrosine motifs are transiently phosphorylated [50-52]. Phospho-Cas-L recruits the adaptor protein Crk-L that is constitutively associated with the guanine exchange factor C3G, which in turn is involved in the activation of the integrin regulating Rap1 GTPase [53-56]. Furthermore, mutational analyses suggest that the substrate domain of Cas-L is required for migration in response to TCR and integrin stimulation [57]. However, the mechanisms leading to assembly of the ternary complex CasL-CrkL-C3G are unknown and whether Cas-L regulates T-cell activation is unclear.

To study T cell activation in the context of the immunological synapse, a system widely used is based on glass supported planar lipid bilayers that mimic the surface of an antigen-presenting cell [5, 58]. Using bilayers, we [11, 13] and others [12] recently reported that Myosin IIa contractility at the immunological synapse is involved in the transport of TCR microclusters, and in sustaining Src-family kinase signals, Ca^{2+} flux, and interleukin-2 (IL-2) secretion. Interestingly, both RNAi depletion and pharmacological inhibition of Myosin IIa activity reduced phosphorylation of Cas-L at the immunological synapse [12, 13]. However, it remains unknown if Cas-L plays a role in the formation of the immunological synapse and how Cas-L integrates initial TCR stimulation events with integrin activation and actomyosin contractility.

The interplay between TCR and integrin signaling is complex and it is unclear how it translates into f-actin polymerization dynamics. A widely established paradigm for integrin signaling studies in T cells is the lymphocyte function activation 1 (LFA-1), a β2 integrin that is critical for immunological synapse formation, and T cell adhesion and activation [59]. TCR stimulation leads to inside-out activation of LFA-1 [60], which undergoes a conformational change into a higher affinity state to bind its ligand ICAM-1 (intercellular adhesion molecule 1) [61]. Interestingly, the strength of the LFA-1/ICAM-1 interaction is regulated by a mechanical feedback loop [62], but whether there is a mechanical link between TCR and LFA-1 remains unknown. However, it is known that activation of Rap1 is critical for LFA-1-mediated T cell adhesion [63, 64], indicating that f-actin based contractility and Cas-L might provide a mechanical connection between TCR and LFA-1.

Among the vast number of molecules that regulate actin polymerization in T cells is the Wiskott-Aldrich Syndrome protein (WASp) [65]. WASp is a multidomain scaffold protein containing binding sites for actin and the Arp2/3 complex, which is an actin nucleation factor responsible

for branching of actin filaments [66]. WASp is recruited to TCR microclusters [67, 68] and can become activated via several pathways [65]. Activated WASp then recruits Arp2/3 complex and initiates actin polymerization from existing filaments. Furthermore, $WASp^{-/-}$ T cells have selective defects in proliferation and IL-2 production [69-71]. Interestingly, we previously reported that WASp favors stability of the immunological synapse [72], and treatment of $WASp^{-/-}$ T cells with an inhibitor of protein kinase C theta (PKCθ) restored immunological synapse stability, suggesting opposing effects within a single pathway for the activity of those two proteins at the immunological synapse.

Here, we wished to determine whether Cas-L plays a role in T cell activation in the context of the immunological synapse using T cells from Cas-L deficient ($Cas\text{-}L^{-/-}$) mice [49]. We report a role for actin polymerization in Cas-L activation at the immunological synapse. In analogy to p130Cas, we hypothesized that a mechanical feedback loop between TCR-mediated Cas-L activation, actin polymerization and LFA-1 activation might regulate the processes of adhesion, migration, and activation of T cells.

Results

Cas-L promotes TCR microcluster translocation

In order to investigate a potential role for Cas-L in T cell activation we measured the accumulation of TCR microclusters and ICAM-1 at the immunological synapse of Cas-L$^{-/-}$ T cells compared with control cells. No Cas-L protein was detected in T cells from Cas-L$^{-/-}$ mice (Figure 1A). We seeded cells on supported lipid bilayers embedded with laterally mobile fluorescently labeled anti-CD3ε and ICAM-1, fixed them after 15 min, imaged them, and plotted the average radial profile of intensities of TCR and ICAM-1 over the entire synapse of both cell types (Figure 1B-C). In control cells, ICAM-1 stays distributed in a pericentral ring at the synapse, but in contrast, ICAM-1 accumulation in Cas-L$^{-/-}$ cells was severely compromised and its pericentral ring organization was lost (Figure 1B blue channel, and Figure 1C blue lines). Further, in Cas-L$^{-/-}$ T cells, accumulation of TCR at the center of the synapse was significantly decreased compared to control cells (Figure 1B red channel, and Figure 1C red lines). Interestingly, a fraction of the TCR microclusters remained arrested at the synapse periphery in Cas-L$^{-/-}$ T cells (Figure 1B red channel). Thus, we asked whether the decreased accumulation of TCR at the immunological synapse of Cas-L$^{-/-}$ T cells was a consequence of deficient transport of TCR microclusters from the periphery to the central domain where extracellular vesicles are formed [16]. In control cells, TCR assembled into microclusters at the periphery of the synapse within seconds of interaction with the bilayer and rapidly moved towards the center, with TCR accumulating in one bright focus at the center of the synapse (Figure 1D top panel; Movie 1 top panel). In contrast, in Cas-L$^{-/-}$ T cells, movement of TCR microclusters towards the center of the synapse was impaired, and approximately 30% of TCR microclusters remained dispersed in the periphery and did not move to the center (Figure 1D bottom panel; Movie 1 bottom panel).

Importantly, in Cas-L$^{-/-}$ T cells, TCR microclusters exhibited a lower speed of translocation (1.92±0.20 μm/min) and a lower mean square displacement (path length 1.78±0.16 μm) than in control cells, where microclusters moved at an average speed of 2.78±0.37 μm/min, with a path length of 2.82±0.38 μm (Figure 1E). Furthermore, we tracked individual TCR microclusters, measured their fluorescence intensities and areas, and plotted the corresponding averages throughout the course of synapse formation (Figure 1F-G). Individual TCR microclusters from Cas-L$^{-/-}$ cells exhibited, on average, decreased intensity and area compared to TCR microclusters from control cells, suggesting that in the absence of Cas-L TCR microclusters have a lower rate of maturation compared to control cells.

Activated Cas-L co-localizes with TCR microclusters at the periphery of the immunological synapse

Since localization of TCR signaling proteins to the immunological synapse correlates with T cell activation, we examined if activation of Cas-L was spatially and temporally coupled to TCR microcluster assembly at the immunological synapse as previously suggested [12]. To assess the level of activation of Cas-L we used an antibody that recognizes phosphorylated tyrosine motifs located in the substrate domain of Cas-L. We seeded cells on anti-CD3ε/ICAM-1-embbeded bilayers, fixed them after 2 minutes, and stained them for phospho-Cas-L (Figure 2A). Importantly, phospho-Cas-L co-localized with nascent TCR microclusters at the periphery of newly-formed synapses (Figure 2A yellow arrows on the bottom-right panel), indicating that

Cas-L phosphorylation is spatially coupled to TCR microcluster assembly at an early stage of immunological synapse formation.

In order to understand how Cas-L becomes activated at TCR microclusters we treated T cells with a small molecule inhibitor of Src-family kinases, PP2 [73]. We found that inhibition of Src-family kinases by PP2 led to a significant decrease in the level of phospho-Cas-L at the immunological synapse (Figure 2B-C). As shown in Figure 2B, in the presence of PP2, the LFA-1 dependent adhesion was nearly completely eliminated, as previously reported [74], but TCR clustering still occurred, suggesting that cell adhesion and Cas-L phosphorylation might be related. The level of phospho-Cas-L at TCR clusters was greatly decreased with PP2 treatment, but as revealed by Pearson's correlation coefficient analysis (Supplemental Figure 1F) the phospho-Cas-L signal was more strongly co-localized with TCR clusters in PP2-treated cells than in the absence of PP2, as TCR clusters were relatively more resistant to inhibition by PP2 compared to LFA-1/ICAM-1 interaction.

We further pursued the relationship between phospho-Cas-L and TCR microclusters. It is known that TCR ligation leads to the recruitment and activation of Src-family kinase Lck, which in turn phosphorylates the immunoreceptor tyrosine-based activation motifs (ITAMs) located on the CD3 chains of the TCR complex [75]. Then, the zeta-chain-associated protein kinase 70 kDa (ZAP70) binds to the doubly phosphorylated zeta-chain ITAMs, exposing phosphorylation sites on its kinase domain activation loop, which in turn are phosphorylated by Lck. Thus, the localization of ZAP70 at TCR microclusters and the phosphorylation status of ZAP70 correlate with TCR activation and Lck activity, respectively. To determine if different baseline levels of TCR activation could account for our observations in Cas-L$^{-/-}$ T cells, we compared the levels of ZAP70 localized to TCR microclusters in both cell types and detected no significant changes

(Supplementary Figure 1A). We also compared the baseline activity levels of the Src-family kinase Lck by probing for the phosphorylated form of ZAP70 (PY319) at TCR microclusters and detected no differences between Cas-L$^{-/-}$ T cells and control cells (Supplementary Figure 1B). Since the baseline levels of TCR activation and Lck activity were not altered in Cas-L$^{-/-}$ T cells compared to control cells, the defects observed in Cas-L$^{-/-}$ T cells were not due to differences in the TCR proximal tyrosine kinase cascade up to ZAP70 recruitment and activation.

Noteworthy, treatment with a selective Lck inhibitor [76] led to a significantly greater decrease in mean intensity levels of phospho-Cas-L than treatment with the selective ZAP70 inhibitor piceatannol [74], suggesting that Cas-L phosphorylation depends on Lck activity (Figure 2D-E).

These results demonstrate that Lck phosphorylates tyrosine residues in the Cas-L substrate domain immediately downstream of TCR stimulation. Thus, while Cas-L is dispensable for the assembly of TCR microclusters, it is required for the efficient transport of newly-formed TCR microclusters to the center of the immunological synapse. Since the centripetal transport of microclusters correlates with sustained TCR signaling [5, 8], these findings suggest that Cas-L might regulate signals downstream of the TCR proximal tyrosine kinase cascade.

Ca^{2+} release from intracellular stores is impaired in Cas-L$^{-/-}$ T cells

Since myosin II dependent transport of TCR microclusters is required to sustain TCR signals in the bilayer model [12, 77, 78], in particular Ca^{2+} signaling, we wanted to determine whether the defective TCR microcluster transport observed in Cas-L$^{-/-}$ T cells was correlated with any defects in Ca^{2+} signaling. To visualize changes in the concentration of free intracellular Ca^{2+}, we loaded cells with the fluorescent Ca^{2+} probe Fluo-4 as described in Materials and Methods. We then

seeded cells on anti-CD3ε/anti-CD28/ICAM-1-coated coverslips and imaged Fluo-4 fluorescence intensity changes (Movie 2). As shown in Figure 3A and plotted in Figure 3B, when cells touched the antibody-coated coverslip they exhibited a sharp increase of Fluo-4 fluorescence intensity corresponding to Ca^{2+} released from intracellular stores, reaching a maximum Fluo-4 fluorescence value (imax1), followed by a decrease of fluorescence intensity down to a sustained lower level, which is dependent upon influx of extracellular Ca^{2+} (Movie 2). The cells were then treated with ionomycin to determine the maximum Fluo-4 fluorescence value (imax2) for scaling, which is important as Fluo-4 loading differs between cells. For each cell the pre-stimulation baseline was set to 0 and the imax2 value was set to 1 and other values normalized accordingly. We observed that Cas-$L^{-/-}$ cells exhibit a lower value of imax1 compared to control cells, but the normalized value of sustained Ca^{2+} was similar in both cell types (Figure 3C-D). Raw values of imax2 in wild type and Cas-$L^{-/-}$ cells were similar suggesting no significant differences in dye loading or Ca^{2+} homeostasis. We also observed that ionomycin quickly halted Cas-$L^{-/-}$ T cell migration, suggesting that the machinery linking Ca^{2+} to migration arrest is intact in the absence of Cas-L (Movie 2 bottom panel). Together these observations suggest that the defect in imax1 Ca^{2+} release observed in Cas-$L^{-/-}$ T cells was due to a TCR-signaling defect.

To gain further insight into the mechanism by which Cas-L reduced Ca^{2+} signaling, we seeded Cas-$L^{-/-}$ T cells and wild type cells on bilayers with anti-CD3ε and ICAM-1 and compared the levels of phosphorylated phospholipase C gamma 1 (PLCγ-1), which generates inositol-1,4,5-trisphosphate required to initiate and sustain Ca^{2+} elevation [79] (Figure 3E). The levels of phospho-PLCγ-1 at TCR microclusters were lower in Cas-$L^{-/-}$ T cells than in control cells (Figure 3F), which provides a plausible mechanism for a role of Cas-L in Ca^{2+} signaling. This defect was

not due to differences in expression level of PLCγ-1, which was similar in wild type and Cas-L$^{-/-}$ cells as analyzed by flow cytometry (data not shown). Although Cas-L$^{-/-}$ CD8^{+} T cells showed impaired Ca^{2+} release and PLCγ1 activation during synapse formation (Figure 3) we saw no significant difference in IL-2 levels between Cas-L$^{-/-}$ and wild type cells during 48h of culture (Supplementary Figure 1C).

Cas-L regulates immunological synapse stability via integrin-mediated adhesion

Seo and colleagues [49] observed that T cells from Cas-L$^{-/-}$ mice exhibit perturbed integrin-mediated adhesion. Integrin-mediated adhesion, namely mediated by LFA-1 ligation by ICAM-1, is critical for immunological synapse formation and enhances sensitivity of T cell activation to MHC-peptide complexes [60]. We showed in Figure 1C that recruitment of ICAM-1 to the immunological synapse was impaired in Cas-L$^{-/-}$ T cells, relative to control cells. Additionally we noticed that although the number of cells seeded on the bilayers was the same for both cell types ($1x10^6$ cells/ml), the population of Cas-L$^{-/-}$ T cells that adhered to the bilayers was significantly decreased in relation to control cells (results not shown). Thus, we wanted to determine whether Cas-L played a role in LFA-1-mediated T cell adhesion by imaging and comparing synapse stability in Cas-L$^{-/-}$ T cells and control cells seeded on bilayers with anti-CD3ε and ICAM-1. We saw that the population of T cells that adhered to the bilayers followed a bimodal distribution, whereby one fraction of the cell population formed stable persistent synapses that remained in the same initial position during the course of the experiment (15min), and another fraction was unstable, and polarized and migrated after contacting the bilayers (Figure 4A; Movie 3). The majority of control cells formed stable synapses, whereas most Cas-L^{-}

$^{/-}$ T cells failed to form a stable synapse, tended to polarize, and migrated in random directions (Figure 4B-C; Movie 3). While more Cas-L$^{-/-}$ T cells migrated than control T cells, the migration speed of Cas-L$^{-/-}$ T cells (3.5±0.51 μm/min) was significantly lower than that of control cells (5.3±0.91 μm/min) (Figure 4C). Furthermore, in contrast to the directionally persistent migration of control cells, Cas-L$^{-/-}$ cells were less persistent, with frequent turns (Movie 3). As a result of their slower migration speed and more frequent turning, Cas-L$^{-/-}$ cells showed smaller displacement, i.e. Cas-L$^{-/-}$ cells travelled shorter distances than control cells in a given time period (Figure 4C). Further, Cas-L$^{-/-}$ T cells revealed defects in early spreading, had significantly smaller synapse area than control cells (Figure 4D), and a larger circularity index (Figure 4E), reflecting their inability to fully spread over the bilayers.

We also measured the levels of ICAM-1 at the synapse throughout the course of these experiments (Figure 4F), and saw impaired ICAM-1 recruitment to the synapse of Cas-L$^{-/-}$ T cells relative to wild type cells. Since ICAM-1 binding to LFA-1 induces high-affinity LFA-1 through outside-in ligand induced conformational changes [74], we hypothesized that if the defects in adhesion, spreading, and synapse stability observed in Cas-L$^{-/-}$ T cells were a consequence of deficient inside-out integrin-signaling mediated by Cas-L, then the number of stable synapses formed by Cas-L$^{-/-}$ T cells should be independent from the concentration of ICAM-1 provided on the bilayers. In fact, bilayers embedded with a constant concentration of anti-CD3ε (above the threshold required to induce T cell activation) and with increasing concentrations of ICAM-1 did not rescue the adhesion defects observed in Cas-L$^{-/-}$ T cells (Figure 4G). While control cells were able to form synapses on bilayers with as low as 30 molecules of ICAM-1 per μm^2, Cas-L$^{-/-}$ cells failed to form stable synapses even over 3-fold the typical level of ICAM-1 (650 molecules of ICAM-1 per μm^2) (Figure 4G). This adhesion defect was not due to lower expression of LFA-1

as the expression levels of LFA-1 were similar in wild type and Cas-L$^{-/-}$ T cells, as analyzed by flow cytometry (Supplementary Figure 1D).

Altogether, these results show that Cas-L plays a role in establishing and maintaining stability of the immunological synapse by promoting inside-out integrin activation leading to T cell adhesion.

Actin polymerization regulates Cas-L activation

In vivo, T cells undergo an extensive search for antigen in lymphoid tissues by using amoeboid migration, a process that requires actin polymerization [80]. The actin cytoskeleton plays, in addition, a critical role in immunological synapse formation and regulation of T cell function [20]. Previous studies using mutational analysis indicated that the substrate domain of Cas-L was required for T cell migration [57], but the mechanism of Cas-L activation was not known. Here, we hypothesize that in a similar way to its paralog p130Cas [34] Cas-L activation depends on actin polymerization. Thus, we looked at how disruption of actin polymerization by cytochalasin D treatment affected phosphorylation levels of Cas-L substrate domain at the immunological synapse. We saw that cytochalasin D induced a strong decrease in the levels of phospho-Cas-L at the synapse compared to DMSO carrier, and its effect was stronger at higher doses (Figure 5A), indicating that phosphorylation of the Cas-L substrate domain depends on actin polymerization.

To further understand the relationship between Cas-L and the actin cytoskeleton, we seeded T cells on bilayers with ant-CD3ε and ICAM-1 and compared f-actin organization in Cas-L$^{-/-}$ cells and control cells. Confocal imaging of fluorescently-labelled phalloidin staining in Cas-L$^{-/-}$ cells revealed a disorganized cortical f-actin network, smaller lamellipodial area, and undefined

lamella/lamellipodia boundaries (Figure 5B). The radial profile of the average f-actin intensity at the synapse also revealed a defective f-actin network in Cas-L$^{-/-}$ cells (Figure 5C), suggesting that Cas-L plays a role in the organization of the structure of the f-actin network. Furthermore, inhibition of the actin polymerization factor Arp2/3 with a small molecular inhibitor (CK666) caused a significant decrease in phospho-Cas-L levels at the immunological synapse compared to DMSO carrier treatment (Figure 5D). Since Arp2/3 also co-localizes with nascent TCR microclusters at the periphery of the synapse [65, 66], this data indicates that Cas-L activation at the TCR microclusters is dependent on the actin polymerization-promoting factor Arp2/3.

To further investigate how actin polymerization regulates Cas-L activation, we asked if WASp [68] played a role in Cas-L activation. We seeded WASp$^{-/-}$ T cells and control cells on bilayers with anti-CD3ε and ICAM-1 and compared their Cas-L phosphorylation levels (Figure 5E). We saw significantly lower levels of phospho-Cas-L at the synapses of WASp$^{-/-}$ T cells compared to control cells. Sims et al [72] previously reported that the roles of WASp and protein kinase C theta (PKCθ) have opposing effects at the immunological synapse, one favoring synapse stability and symmetry, the other promoting polarization and migration, respectively. Hence, we investigated whether the increased migration observed in Cas-L$^{-/-}$ cells was due to PKCθ driven symmetry breaking. In fact, when we treated Cas-L$^{-/-}$ T-cells with an inhibitor of PKCθ activity, we saw that Cas-L$^{-/-}$ cells formed significantly more stable synapses compared to DMSO-treated Cas-L$^{-/-}$ cells (Figure 5F), suggesting that Cas-L is part of the WASp dependent synapse stabilizing machinery that is opposed by PKCθ activity. Consistent with this observation, in previous studies [72], the same PKC inhibitor led to a reduction in the migration speed of WASp$^{-/-}$ T cells and wild type cells. Altogether, our results are consistent with the model that actin

polymerization-dependent Cas-L phosphorylation at TCR microclusters contributes to immunological synapse formation and is important for immunological synapse stability.

Discussion

Building an immunological synapse provides a mechanism to assess sensitivity and specificity of the interaction between antigen and TCR. The intrinsically transient TCR-MHC-peptide interaction is organized into clusters that are subjected to physical forces associated with transport as a critical determinant of T cell signaling. These dynamic processes take place in stable immunological synapse to allow for signal integration and effector functions [80]. Generation of effective recall response may be particularly reliant on stable immunological synapses [81].

Our results here show that Cas-L is involved in stabilizing the immunological synapse and establishing synapse symmetry. Furthermore, we show that Cas-L is necessary for efficient transport of TCR microclusters from the periphery to the center of the synapse, and without Cas-L, microcluster translocation slows down or is completely arrested. Our findings reveal that both activation of phospho-Cas-L localizes to early TCR microclusters where tyrosine phosphorylation and WASp dependent actin polymerization occur [9, 18]. We found that disrupting actin polymerization with cytochalasin D or inhibiting actin nucleation factor Arp2/3 led to a significant decrease in phospho-Cas-L levels at TCR microclusters. Finally, we propose a new role for Cas-L as a mechanical link bridging f-actin foci at TCR microclusters, as well as at the lamellipodial f-actin ring facilitated by LFA-1/ICAM-1 dependent adhesion.

Stable immunological synapses are not required for T cell proliferation, but appear to be critical for asymmetric cell division and functional memory [80-82]. In vivo analyses with tracking of single T cells by bar-coding have challenged the need for asymmetric division as a drive, but still demonstrate striking heterogeneity in the behavior of individual T cell clones, which may rely on

a spectrum of interactions including stable immunological synapses [83]. It has also been proposed that synapse stabilization in vivo may help T cells of lower affinities for an antigen decide whether or not to participate in a response [84]. In particular for a T cell effector response, the initial free intracellular Ca^{2+} spike (imax1) is critical for rapid arrest of migrating cells and direct cell-cell communication that establishes that response. Here, we saw that Cas-$L^{-/-}$ $CD8^{+}$ T cells release only approximately half of their total Ca^{2+} reserves, which amounts to a decrease of approximately 30% compared to wild type cells. Remarkably, the proportion of Cas-$L^{-/-}$ T cells that adhered to anti-CD3ε/ICAM1-embedded supported planar bilayers was only half of that of control cells, and they had a smaller contact area compared to control cells. Furthermore, Cas-$L^{-/-}$ cells formed unstable synapses that failed to remain symmetric, exhibiting irregular lamellipodial ruffling, and uncoordinated migration. This phenotype might be explained by the defects we saw in the actin cytoskeleton of Cas-$L^{-/-}$ T cells, which exhibited a disordered cortical f-actin network, and lost the defined border between lamella and lamellipodia structures. Additionally, studies have shown that the size of TCR microclusters correlates with T cell activation [6]. Here, we saw that immunological synapses formed by Cas-$L^{-/-}$ T cells showed a decreased accumulation of TCR in the central region and the size of microclusters was smaller compared to control cells. Altogether, these data suggest that Cas-L might be important for T cell survival and proliferation [81, 82, 84] by establishing immunological synapse stability.

In an effort to understand the mechanism by which Cas-L establishes immunological synapse stability, we looked into a model we previously reported [72] describing how T cells regulate synapse symmetry and migration. There we demonstrated that PKCθ activity promotes synapse symmetry breaking leading to migration, whereas WASp activity favors synapse symmetry and promotes synapse stability. In line with those studies, here we saw that inhibition of

PKCθ activity in Cas-L$^{-/-}$ T cells impeded migration and restored synapse stability. Furthermore, activated phospho-Cas-L at TCR microclusters was decreased in WASp$^{-/-}$ T cells, suggesting that Cas-L activation at TCR microclusters is dependent on WASp activity. Altogether, these data further corroborate a role for Cas-L in promoting synapse symmetry and stability.

Despite functioning downstream of WASp and actin polymerization at TCR clusters, Cas-L also contributes to the proper organization of the peripheral f-actin ring in defining the lamella/lamellipodia regions, which suggests that Cas-L is part of a feedback loop mechanism favoring TCR signal amplification and immunological synapse stability. Our co-localization analysis (Supplemental Figure 1F) suggests that both the TCR microcluster actin foci and the lamellipodial f-actin ring that is facilitated by LFA-1-ICAM-1 interaction contribute to phospho-Cas-L activation. It is known that ligation of TCR causes recruitment of active Lck, and recruitment and activation of WASp via the WIP-CrkL pathway, which in turn recruits Arp2/3, thus triggering actin-polymerization [65-68]. Since phospho-Cas-L associates strongly with Crk-L [50, 52] it is plausible to hypothesize that Cas-L is part of a multiprotein complex comprising Cas-Crk-C3G-Rap1, thus leading to activation of LFA-1-dependent adhesion through effectors including RapL and RIAM [63, 85-88]. In addition, previous studies [89] show that the proline-rich tyrosine kinase 2 (Pyk2) associates with LFA-1 and it is essential for CD8^{+} T cell adhesion and migration. Pyk2 has been reported to phosphorylate Cas-L [90], and unpublished data from Sheetz lab suggests that Cas-L might form a complex with Pyk2 and LFA-1 that could work as a physical link connecting TCR clusters, LFA-1, and the actin cytoskeleton.

Moreover, Cas-L might also be involved in Rap1 activation, integrin-mediated adhesion, and f-actin polymerization by associating with the adaptor protein Chat-H, thus forming a complex that has previously been implicated in integrin-mediated adhesion and naïve T cell migration in

response to TCR stimulation [91, 92]. In those studies, RNAi-mediated knockdown of Chat-H resulted in impaired Rap1 activation, integrin-mediated adhesion, and T cell migration [91]. Those results are in line with our model and support a role for the Cas-L/Chat-H complex as an early regulator of T cell adhesion and migration upstream of Rap1 in response to TCR stimulation.

It is known that upon TCR stimulation, ZAP70, a kinase important for TCR-mediated signaling leading to Ca^{2+} flux and IL-2 production, is recruited to the phosphorylated ITAMs on the zeta chains of the CD3ε subunit of TCR. Then, ZAP70 phosphorylates adaptor proteins LAT and SLP76, which in turn recruit PLCγ1 [32, 68, 93]. Subsequently, PLCγ1 cleaves PIP2, generating IP3 and DAG, which lead to Ca^{2+} release, and PKCθ activation and Ras activation, respectively [93]. PLCγ-1 activation is a critical step in TCR signaling that requires the function of the TCR proximal tyrosine kinase cascade and links it to rapid release of Ca^{2+} from intracellular stores. Here, we saw that Cas-$L^{-/-}$ $CD8^{+}$ T cells have a significant defect in Ca^{2+} release in response to TCR stimulation. This defect was accompanied by decreased levels of phospho-PLCγ-1 at the immunological synapses of Cas-$L^{-/-}$ T cells relatively to the control, supporting a role for Cas-L in the amplification of TCR signals that ultimately lead to T cell activation.

In order to see whether the absence of Cas-L had an effect on signaling steps further downstream of TCR stimulation, we compared the levels of IL-2 production in Cas-$L^{-/-}$ and wild type T cells and saw no significant difference in IL-2 production. Consistent with this observation, we showed that pharmacological inhibition of ZAP70 had a minor effect on phospho-Cas-L levels. In line with these results, previous studies [94] have also shown that disruption of f-actin polymerization reduced levels of phospho-PLCγ1 within TCR microclusters without affecting ZAP70 activity. These observations suggest that alternative pathways downstream of ZAP70 take place independently of Cas-L activation.

Additionally, the molecular events leading to Cas-L activation take place at a different stage and time scale than the events leading to IL-2 expression and secretion. In fact, while Cas-L recruitment and phosphorylation at the TCR microclusters is transient, occurring in the first 2-5 minutes of synapse formation and then dropping, IL-2 production takes place at later stages, 24h-48h after synapse formation. Thus, Cas-L seems to play a particularly important role at early stages, while WASp has a broader role such that IL-2 production is lower in $WASp^{-/-}$ T cells [71], perhaps due to structurally distinct TCR-mediated signaling events that are not as dependent upon Cas-L. Nevertheless, we provide clear evidence that $Cas\text{-}L^{-/-}$ T cells show impaired early Ca^{2+} signaling compared to wild type cells, demonstrating a role for Cas-L in TCR-mediated signaling and in regulating immunological synapse stability.

Recent studies in $WASP^{-/-}$ T cells reveal that TCR microcluster associated f-actin foci play an important role of PLC-γ activation without having any effect on the TCR proximal tyrosine kinase cascade [95]. While WASP dependent f-actin foci were closely associated with TCR signaling, phosphorylation of Cas-L was only weakly impacted by inhibition of ZAP-70 catalytic activity, which is also a characteristic of LFA-1 regulation downstream of the TCR [96]. Altogether these data suggest that WASp dependent activation of Cas-L by TCR microcluster associated f-actin likely plays an important role in the initiation and maintenance of TCR signaling.

The guanine nucleotide exchange factor DOCK2 is found associated with Crk-L in leukemia cell lines [97], which in turn binds phospho-Cas-L via its SH2 domain downstream of TCR activation [50, 52]. Thus, we speculate that a CasL-CrkL-DOCK2-Rac multiprotein complex can that directly activate the small GTPase Rac downstream of TCR activation, thus promoting f-actin polymerization through activation of the WAVE2 complex [97-99]. Cas-L is part of a multiprotein complex comprising Cas-Crk-C3G-Rap1, thus leading to activation of LFA-1-dependent

adhesion through effectors including RapL and RIAM Furthermore, a recent study [100] reported that while early TCR microclusters are able to activate T cell cytokine expression, centralization of TCR microclusters is more important for Notch-ADAM10-Vav1-dependent T cell proliferation. It is possible that the role of Cas-L in the centripetal movement of TCR microclusters at the immunological synapse might be more relevant for the signaling pathway leading to T cell proliferation than to cytokine production. Hence, Cas-L may play distinct roles in different signaling pathways leading to cytokine production and T cell proliferation, thus providing alternative regulation mechanisms for the TCR signaling events that ultimately lead to IL-2 production and T cell-mediated immune responses.

Accumulation of ICAM-1 at the immunological synapse is rapidly initiated and then sustained for many minutes even when TCR signaling is selectively blocked [9]. However, we saw that accumulation of ICAM-1 at the synapses of Cas-L$^{-/-}$ T cells was impaired, suggesting a potential role for Cas-L-mediated integrin activation. Surprisingly, using bilayers with increasing amounts of ICAM-1 (and a fixed amount of anti-CD3ε antibody) did not rescue spreading defects in Cas-L$^{-/-}$ T cells. These were particular interesting results since in control cells as few as 30 molecules of ICAM-1 per μm^2 were sufficient to allow synapse formation, whereas increasing to 650 molecules of ICAM-1 per μm^2 was insufficient. The ability of Cas-L deficient T cells to form a few synapses, rather than none, may be a result of TCR and Cas-L independent activation of integrins [101, 102].

Our observations here are in line with recent studies we [11, 13] and others [12] reported on the role of myosin-IIa activity in immunological synapse formation and Cas-L activation. In those studies, inhibition of myosin-IIA activity or myosin IIA knockdown activity led to a decrease, but not complete elimination, in phospho-Cas-L levels. Thus, those results supported a two-step model

in which initial TCR ligation, activation of Lck, assembly of TCR microclusters, initial activation of Cas-L, and recruitment of myosin IIA are all independent of myosin IIA activity, whereas amplification of Cas-L phosphorylation and microcluster transport are dependent on myosin IIA activity.

We can now develop a working model for the role for Cas-L as a link between TCR, actin, and integrins (Figure 6). We previously described a model for actin polymerization-dependent stretch of p130Cas leading to cell adhesion and migration via activation of the regulator of actin-polymerization Rap1 [34]. Here, we propose that actin polymerization triggered by TCR proximal signals involving WASp activates Cas-L by exposing cryptic tyrosine residues in its substrate domain, which then are phosphorylated by Src-family kinases, in particular Lck. Phospho-Cas-L then recruits SH2-containing proteins and other signaling factors that promote further TCR clustering. TCR signaling immediately downstream of these clusters drives the onset of Ca^{2+} release, and Calmodulin-mediated MLCK activation, which in turn activates myosin-IIa contraction. Then, actomyosin contractility at the periphery contributes to TCR cluster transport, acting via a positive feedback loop that further activates Cas-L, integrin adhesion, and lamellipodia formation, and that ultimately leads immunological synapse formation and conditions required for induction of memory T cells.

In Cas-$L^{-/-}$ T cells the link between TCR-induced Ca^{2+} signaling and integrin activation seems to be broken and consequently cells are unable to form stable synapses independently of the amount of ICAM-1 provided. Thus, it is plausible to hypothesize that Cas-L is part of a multi-protein complex that links TCR proximal actin polymerization to LFA-1 activation and Cas-$L^{-/-}$ T cells have unstable synapses in part due to loss of this connection. This is not simply a matter of LFA-1 affinity as the defect cannot be rescued with high ICAM-1. These synapse defects may

manifest as defective memory and effector function, thus explaining the in vivo defects observed in Cas-L$^{-/-}$ mice by Seo et al [49].

Despite the striking morphological and functional differences between fibroblasts and T cells, here we demonstrate through the Cas model that the fundamental principles of mechanotransduction are evolutionarily conserved across different cell types [34, 103].

Methods

Cells and culture conditions

Cas-L$^{-/-}$ mice on the C57BL6 background [49] were maintained in a specific pathogen free facility at MSSM under the supervision of the institutional animal care and use committee. Naïve CD8^{+} T cells were isolated from the spleens of Cas-L$^{-/-}$ mice and their wild type littermates using the Dynal negative isolation (Invitrogen) following the manufacturer's protocol. Briefly, splenocytes were incubated with a mixture of antibodies against the CD8-negative T cells, and then incubated with superparamagnetic polystyrene beads coated with a polyclonal sheep anti-rat IgG antibody. Then, the bead-bound cells were separated by a magnet, and the remaining untouched CD8^{+} T cells were used for the experiments described here.

All experiments were performed in primary murine lymphocytes from the spleen, freshly isolated from mice about the same age (6-10 weeks), and enriched for CD8^{+} T cells using a standard negative selection procedure, yielding a population purity of 95%-97%, as measured by flow cytometry (data not shown). Quiescent T cell populations comprised a mixture of naïve, memory, and effector T cells, as measured by the levels of CD62L$^{high/low}$, and CD127$^{+/-}$ (data not shown).

Cell culture medium was RPMI 1640 (Sigma or GIBCO, NY) with 10% heat-inactivated fetal calf serum (FCS; Life Technologies GIBCO, NY). Cells were kept in a 37 ˚C, 5% CO_2 humidified incubator.

Glass-supported lipid bilayer assembly

To recreate early events at the immunological synapse between a T cell with an antigen-presenting cell in real-time we prepared planar lipid bilayers embedded with fluorescently labeled ligands to engage key T cell surface receptors: 2C11 mAb against TCR/CD3ε and ICAM-1 at 35 molecules/μm^2 and 150 molecules/μm^2, respectively. Planar lipid bilayers provide a valid model for studying immunological synapse formation dynamics by high resolution microscopy, faithfully reconstituting the supramolecular organization of the T cell/APC interface previously described [5, 58]. The bilayer-presented TCR and LFA-1 ligands can move freely throughout the plane of the bilayers, and we labeled them with different fluorophores to allow high-resolution spatio-temporal characterization of immunological synapse formation. To validate the quality of the bilayers, we tested the lateral mobility of the ligands by recording their fluorescence recovery after photobleaching (FRAP) kinetics before seeding cells. In all experiments, we use fresh primary $CD8^+$ T cells purified by negative selection from spleen of Cas-$L^{-/-}$ mice or their wild type littermates.

Supported planar bilayers were assembled in parallel plate flow cells (Bioptechs or Ibidi) from unilamellar vesicles containing 12% mol% 1,2-dioleoyl-sn-glycero-3-[(N-(5-amino-1-carboxypentyl)-iminodiacetic acid)-succinyl] (nickel salt), 0.01 mol% 1,2-dioleoyl-sn-glycero-3-phosphoethanolamine-N-(capbiotinyl), and 87.99% mol% 1-oleoyl-2-palmitoyl-phosphatidylcholine (Avanti Polar Lipids). Bilayers were loaded with monobiotinylated-564-2C11 mouse antibody prepared as described [104]. Non-specific binding was reduced by blocking with 5% casein in PBS. Cells were allowed to settle and form contacts with the bilayer during imaging.

The estimate of the number of molecules of ICAM-1 on the bilayers was performed on an independent assay using bilayers on glass beads as described elsewhere [58].

Microscopy

TIRF imaging was carried out using a Nikon Eclipse Ti with 60X N.A. 1.49 objective and an Andor DU897 back illuminated EMCCD camera. Solid-state lasers (Coherent) provided illumination at 488, 561 and 641 nm and narrow pass filters (Chroma Technology) were used for detection. Widefield epi-illumination for Ca^{2+} imaging was provided by a 150 W Xe lamp on an Olympus IX70 with a Zeiss 40x 1.3NA Fluar objective, Ludl filter wheels and a Hamamatsu 12-bit C9100 1.1B charge-coupled device. Acquisition settings were maintained constant throughout each imaging procedure and between samples. Image analysis was performed with Metamorph and ImageJ. Briefly, to measure intensities, images were subtracted for background, then cells in the subtracted images were marked with ROIs, and the intensity values obtained from the ROIs were plotted as raw values in scatter plots, unless otherwise indicated. The graphs and statistical analyses were performed with Microsoft Excel and Graphpad Prism, and p-values were calculated using two-tailed unpaired Student's t-test if the data were normally distributed or Mann-Whitney if data were not normally distributed. Data sets were tested for normal distribution using the Shapiro-Wilk test. Two tailed Student's t-test was used for comparison between two groups. Microcluster tracking was performed with Volocity 4.2 (Improvision).

Image analysis

The cell boundaries were defined in ImageJ using the "Magic wand" tool after making the images binary with the "Threshold" function. The "Magic wand" tool uses an algorithm that selects all connected pixels above the lower and below the upper threshold values (or value 1 in

the case of a binary image), which were set based on the image background and pixel saturation, respectively. To obtain a coherent mask of the cells, the functions "Close", "Fill Holes" and "Remove Outliers" were also used when necessary. Each cell was added to a list using "ROI Manager", and then measurements of area and mean intensity were compiled. Our method to define cell boundaries involved using the program CellProfiler [105], setting a threshold intensity mask in one of the channels to identify the whole synapse area, and setting another mask on the other channel to identify TCR microclusters. Thus, we were able to measure total or mean fluorescence intensity of proteins over the whole synapse area, or just over the TCR clusters only. Using the masks defined in CellProfiler we computed the Pearson's correlation coefficient to quantify the overlap between phospho-Cas-L and TCR over the whole synapse area or just over the TCR clusters only. The Pearson's coefficient was then plotted to compare signal co-localization.

Intracellular Ca^{2+} detection

We tracked spreading cells by internal reflection microscopy (IRM) and used a Ca^{2+}-specific fluorescent probe (Fluo4-AM, Molecular Probes F14217) to detect variations of Ca^{2+} levels with epifluorescence. The Fluo-4-AM Ca^{2+} dye was dissolved in DMSO at 5 mM (1000X) and Pluronic (Molecular Probes P3000MP) was added at 50 mg/ml to aid the solubilization of the dye into aqueous buffers. Cells were pelleted by centrifuging at 200 × g (1,250 rpm) for 5 min at 4˚C, and the pellet was resuspended in 1 ml HBS/1%HSA. The freshly made Fluo-4/DMSO/Pluronic solution was added to the cell suspension to achieve a 5 µM final Fluo4-AM concentration, and incubated 30 min at room temperature, to allow efficient uptake and de-

esterification of the AM esters from the dye. Finally, cells were washed with PBS, pelleted, and resuspended in phenol free HBS/1%HSA. As a measurement of the relative changes in free intracellular Ca^{2+}, raw values of total fluorescence intensity for each cell were background corrected and normalized to the maximum intracellular Ca^{2+} release measured after addition to the medium of ionomycin (1 µM), an ionophore that releases Ca^{2+} from intracellular stores. The acquisition rate was 16 frames/min for the long term acquisition.

IL-2 production measurement

Freshly isolated Cas-$L^{-/-}$ or control mouse splenic $CD8^+$ T cells ($1x10^5$ cells) were cultured in 200 µl RPMI medium with 10% FCS for 48h on glass chambers coated with anti-CD3ε antibody and ICAM-1 (both at 5 µg/ml), or uncoated chambers as unstimulated (negative) control. Cell culture supernatant was collected at 6h, 12h, 24h, or 48h of culture, centrifuged to remove cells and debris, and stored at -20˚C until analysis. IL-2 concentration in the supernatant was determined using a standard ELISA kit for mouse IL-2 (Invitrogen). A plate reader was used to measure 450 nm absorbance of each well, and a standard curve was plotted with a second order polynomial fit.

Pharmacological perturbations

The Src-family kinase inhibitor PP2 [73] was added to $1x10^6$ cells in 100 µl at a final concentration of 10 µM, incubated for 15 min at 37 ˚C, and added to the bilayers. Treatments with Lck inhibitor (10 µM; [76]), Lck and Syk-family inhibitor Piceatannol (10 µM; [74]), protein kinase C

theta inhibitor C20 (10 μM or 33 μM; [72]), Arp2/3 inhibitor CK666 (10 μM), and actin polymerization inhibitor cytochalasin D (60 nM or 200 nM) followed similar protocol described for PP2. All inhibitors were dissolved in DMSO, and all pharmacological experiments performed included a DMSO only incubation control.

Immunocytochemistry

After incubating cells for 3 min at 37 ˚C, cells were fixed with 2% para-formaldehyde, and permeabilized with 0.01% Triton-X in PBS for 2 min, followed by blocking with 5% casein for 30 min. Primary antibody incubation was performed overnight at 4 ˚C, followed by fluorescently labeled secondary antibody incubation (with or without Phalloidin) for 1 hour at room temperature. Primary antibodies used: Cas-L (clone 2G9; Novus Biologicals #NB100-1699); phospho-Cas-L (Cell Signaling #4015); ZAP70 (clone 99F2; Cell Signaling #2705); phospho-ZAP70 (Tyr319; Cell Signaling #2701). Fluorescently labeled secondary antibodies were obtained from Molecular Probes.

Sodium dodecylsulfate polyacrylamide gel electrophoresis (SDS-PAGE) and immunoblotting

Cells ($1x10^6$ in 100 μl of RPMI 1640 complete medium) were incubated with pharmacological agents as indicated for 15 min prior to seeding on anti-CD3ε/anti-CD28/ICAM-1-coated glass coverslip. After 5 min of interaction with the coverslip cells were lysed with RIPA buffer, solubilized in Laemmli sample buffer supplemented with 5% beta-mercaptoethanol, boiled, and

stored at -70 ˚C. Samples were run on a gradient (4%-20%) SDS-PAGE and transferred to a nitrocellulose membrane, blocked, incubated overnight with primary antibody, washed, incubated for 1h with horseradish peroxidase (HRP)-labelled secondary antibodies and immunoreactivity was visualized by chemiluminescence detection with film. Relative quantification of protein levels was performed from intensity measurements of the bands on the membrane images using ImageJ "Measurements/Intensity" tool after inversion of the lookup table to generate positive values.

Acknowledgments

We thank Sachiko Seo for developing and kindly providing the Cas-L deficient mice. We thank Elena Pugacheva, Geraldine O'Neill, and Erica Golemis for generously providing CasL antibodies, constructs, and accurate insight on CasL structure and function. We thank Xian Zhang for valuable insight on p130Cas function. We thank Meehan Crist for editing the manuscript. We thank the Nanomedicine Center for helpful discussions and useful suggestions.

Conflict of Interest

The authors declare no conflict of interest.

References

1. Crabtree GR. Contingent genetic regulatory events in T lymphocyte activation. *Science* 1989; **243**(4889)**:** 355-61.

2. Weiss A. Molecular and genetic insights into T cell antigen receptor structure and function. *Annu Rev Genet* 1991; **25:** 487-510.

3. Paul WE, Seder RA. Lymphocyte responses and cytokines. *Cell* 1994; **76**(2)**:** 241-51.

4. Dustin ML, Miller JM, Ranganath S, Vignali DA, Viner NJ, Nelson CA *et al.* TCR-mediated adhesion of T cell hybridomas to planar bilayers containing purified MHC class II/peptide complexes and receptor shedding during detachment. *J Immunol* 1996; **157**(5)**:** 2014-21.

5. Monks CR, Freiberg BA, Kupfer H, Sciaky N, Kupfer A. Three-dimensional segregation of supramolecular activation clusters in T cells. *Nature* 1998; **395**(6697)**:** 82-6.

6. Grakoui A, Bromley SK, Sumen C, Davis MM, Shaw AS, Allen PM *et al.* The immunological synapse: a molecular machine controlling T cell activation. *Science* 1999; **285**(5425)**:** 221-7.

7. Davis DM, Dustin ML. What is the importance of the immunological synapse? *Trends Immunol* 2004; **25**(6)**:** 323-7.

8. Lee KH, Dinner AR, Tu C, Campi G, Raychaudhuri S, Varma R *et al.* The immunological synapse balances T cell receptor signaling and degradation. *Science* 2003; **302**(5648)**:** 1218-22.

9. Varma R, Campi G, Yokosuka T, Saito T, Dustin ML. T cell receptor-proximal signals are sustained in peripheral microclusters and terminated in the central supramolecular activation cluster. *Immunity* 2006; **25**(1)**:** 117-27.

10. Kaizuka Y, Douglass AD, Varma R, Dustin ML, Vale RD. Mechanisms for segregating T cell receptor and adhesion molecules during immunological synapse formation in Jurkat T cells. *Proc Natl Acad Sci U S A* 2007; **104**(51)**:** 20296-301.

11. Ilani T, Vasiliver-Shamis G, Vardhana S, Bretscher A, Dustin ML. T cell antigen receptor signaling and immunological synapse stability require myosin IIA. *Nat Immunol* 2009; **10**(5)**:** 531-9.

12. Yu Y, Fay NC, Smoligovets AA, Wu HJ, Groves JT. Myosin IIA modulates T cell receptor transport and CasL phosphorylation during early immunological synapse formation. *PLoS One* 2012; **7**(2)**:** e30704.

13. Kumari S, Vardhana S, Cammer M, Curado S, Santos L, Sheetz MP *et al.* T Lymphocyte Myosin IIA is Required for Maturation of the Immunological Synapse. *Front Immunol* 2012; **3:** 230.

14. Hashimoto-Tane A, Yokosuka T, Sakata-Sogawa K, Sakuma M, Ishihara C, Tokunaga M *et al.* Dynein-driven transport of T cell receptor microclusters regulates immune synapse formation and T cell activation. *Immunity* 2011; **34**(6)**:** 919-31.

15. Vardhana S, Choudhuri K, Varma R, Dustin ML. Essential role of ubiquitin and TSG101 protein in formation and function of the central supramolecular activation cluster. *Immunity* 2010; **32**(4)**:** 531-40.

16. Choudhuri K, Llodra J, Roth EW, Tsai J, Gordo S, Wucherpfennig KW *et al.* Polarized release of T-cell-receptor-enriched microvesicles at the immunological synapse. *Nature* 2014; **507**(7490)**:** 118-23.

17. Dustin ML, Olszowy MW, Holdorf AD, Li J, Bromley S, Desai N *et al.* A novel adaptor protein orchestrates receptor patterning and cytoskeletal polarity in T-cell contacts. *Cell* 1998; **94**(5)**:** 667-77.

18. Campi G, Varma R, Dustin ML. Actin and agonist MHC-peptide complex-dependent T cell receptor microclusters as scaffolds for signaling. *J Exp Med* 2005; **202**(8)**:** 1031-6.

19. Kumari S, Curado S, Mayya V, Dustin ML. T cell antigen receptor activation and actin cytoskeleton remodeling. *Biochim Biophys Acta* 2013.

20. Piragyte I, Jun CD. Actin engine in immunological synapse. *Immune Netw* 2012; **12**(3)**:** 71-83.

21. Bubeck Wardenburg J, Pappu R, Bu JY, Mayer B, Chernoff J, Straus D *et al.* Regulation of PAK activation and the T cell cytoskeleton by the linker protein SLP-76. *Immunity* 1998; **9**(5)**:** 607-16.

22. Bunnell SC, Hong DI, Kardon JR, Yamazaki T, McGlade CJ, Barr VA *et al.* T cell receptor ligation induces the formation of dynamically regulated signaling assemblies. *J Cell Biol* 2002; **158**(7)**:** 1263-75.

23. Dustin ML, Groves JT. Receptor signaling clusters in the immune synapse. *Annu Rev Biophys* 2012; **41:** 543-56.

24. Reich Z, Boniface JJ, Lyons DS, Borochov N, Wachtel EJ, Davis MM. Ligand-specific oligomerization of T-cell receptor molecules. *Nature* 1997; **387**(6633)**:** 617-20.

25. Bray D, Levin MD, Morton-Firth CJ. Receptor clustering as a cellular mechanism to control sensitivity. *Nature* 1998; **393**(6680)**:** 85-8.

26. Mossman KD, Campi G, Groves JT, Dustin ML. Altered TCR signaling from geometrically repatterned immunological synapses. *Science* 2005; **310**(5751)**:** 1191-3.

27. DeMond AL, Mossman KD, Starr T, Dustin ML, Groves JT. T cell receptor microcluster transport through molecular mazes reveals mechanism of translocation. *Biophys J* 2008; **94**(8)**:** 3286-92.

28. Kim ST, Takeuchi K, Sun ZY, Touma M, Castro CE, Fahmy A *et al.* The alphabeta T cell receptor is an anisotropic mechanosensor. *J Biol Chem* 2009; **284**(45)**:** 31028-37.

29. Li YC, Chen BM, Wu PC, Cheng TL, Kao LS, Tao MH *et al.* Cutting Edge: mechanical forces acting on T cells immobilized via the TCR complex can trigger TCR signaling. *J Immunol* 2010; **184**(11)**:** 5959-63.

30. Husson J, Chemin K, Bohineust A, Hivroz C, Henry N. Force generation upon T cell receptor engagement. *PLoS One* 2011; **6**(5)**:** e19680.

31. Judokusumo E, Tabdanov E, Kumari S, Dustin ML, Kam LC. Mechanosensing in T lymphocyte activation. *Biophys J* 2012; **102**(2)**:** L5-7.

32. Jordan MS, Singer AL, Koretzky GA. Adaptors as central mediators of signal transduction in immune cells. *Nat Immunol* 2003; **4**(2)**:** 110-6.

33. Sakai R, Iwamatsu A, Hirano N, Ogawa S, Tanaka T, Mano H *et al.* A novel signaling molecule, p130, forms stable complexes in vivo with v-Crk and v-Src in a tyrosine phosphorylation-dependent manner. *Embo J* 1994; **13**(16)**:** 3748-56.

34. Sawada Y, Tamada M, Dubin-Thaler BJ, Cherniavskaya O, Sakai R, Tanaka S *et al.* Force sensing by mechanical extension of the Src family kinase substrate p130Cas. *Cell* 2006; **127**(5)**:** 1015-26.

35. Kostic A, Sheetz MP. Fibronectin rigidity response through Fyn and p130Cas recruitment to the leading edge. *Mol Biol Cell* 2006; **17**(6)**:** 2684-95.

36. Kostic A, Sap J, Sheetz MP. RPTPalpha is required for rigidity-dependent inhibition of extension and differentiation of hippocampal neurons. *J Cell Sci* 2007; **120**(Pt 21)**:** 3895-904.

37. Tamada M, Sheetz MP, Sawada Y. Activation of a signaling cascade by cytoskeleton stretch. *Dev Cell* 2004; **7**(5)**:** 709-18.

38. O'Neill GM, Fashena SJ, Golemis EA. Integrin signalling: a new Cas(t) of characters enters the stage. *Trends Cell Biol* 2000; **10**(3)**:** 111-9.

39. Minegishi M, Tachibana K, Sato T, Iwata S, Nojima Y, Morimoto C. Structure and function of Cas-L, a 105-kD Crk-associated substrate-related protein that is involved in beta 1 integrin-mediated signaling in lymphocytes. *J Exp Med* 1996; **184**(4)**:** 1365-75.

40. Seo S, Ichikawa M, Kurokawa M. Structure and function of cas-L and integrin-mediated signaling. *Crit Rev Immunol* 2006; **26**(5)**:** 391-406.

41. O'Neill GM, Seo S, Serebriiskii IG, Lessin SR, Golemis EA. A new central scaffold for metastasis: parsing HEF1/Cas-L/NEDD9. *Cancer Res* 2007; **67**(19)**:** 8975-9.

42. Pugacheva EN, Jablonski SA, Hartman TR, Henske EP, Golemis EA. HEF1-dependent Aurora A activation induces disassembly of the primary cilium. *Cell* 2007; **129**(7)**:** 1351-63.

43. Izumchenko E, Singh MK, Plotnikova OV, Tikhmyanova N, Little JL, Serebriiskii IG *et al.* NEDD9 promotes oncogenic signaling in mammary tumor development. *Cancer Res* 2009; **69**(18)**:** 7198-206.

44. Li Y, Bavarva JH, Wang Z, Guo J, Qian C, Thibodeau SN *et al.* HEF1, a novel target of Wnt signaling, promotes colonic cell migration and cancer progression. *Oncogene* 2011; **30**(23)**:** 2633-43.

45. Miyake-Nishijima R, Iwata S, Saijo S, Kobayashi H, Kobayashi S, Souta-Kuribara A *et al.* Role of Crk-associated substrate lymphocyte type in the pathophysiology of rheumatoid arthritis in tax transgenic mice and in humans. *Arthritis Rheum* 2003; **48**(7)**:** 1890-900.

46. Sasaki T, Iwata S, Okano HJ, Urasaki Y, Hamada J, Tanaka H *et al.* Nedd9 protein, a Cas-L homologue, is upregulated after transient global ischemia in rats: possible involvement of Nedd9 in the differentiation of neurons after ischemia. *Stroke* 2005; **36**(11)**:** 2457-62.

47. Aquino JB, Lallemend F, Marmigere F, Adameyko, II, Golemis EA, Ernfors P. The retinoic acid inducible Cas-family signaling protein Nedd9 regulates neural crest cell migration by modulating adhesion and actin dynamics. *Neuroscience* 2009; **162**(4)**:** 1106-19.

48. Vogel V, Sheetz M. Local force and geometry sensing regulate cell functions. *Nat Rev Mol Cell Biol* 2006; **7**(4)**:** 265-75.

49. Seo S, Asai T, Saito T, Suzuki T, Morishita Y, Nakamoto T *et al.* Crk-associated substrate lymphocyte type is required for lymphocyte trafficking and marginal zone B cell maintenance. *J Immunol* 2005; **175**(6)**:** 3492-501.

50. Astier A, Manie SN, Law SF, Canty T, Haghayghi N, Druker BJ *et al.* Association of the Cas-like molecule HEF1 with CrkL following integrin and antigen receptor signaling in human B-cells: potential relevance to neoplastic lymphohematopoietic cells. *Leuk Lymphoma* 1997; **28**(1-2)**:** 65-72.

51. Kanda H, Mimura T, Morino N, Hamasaki K, Nakamoto T, Hirai H *et al.* Ligation of the T cell antigen receptor induces tyrosine phosphorylation of p105CasL, a member of the p130Cas-related docking protein family, and its subsequent binding to the Src homology 2 domain of c-Crk. *Eur J Immunol* 1997; **27**(8)**:** 2113-7.

52. Ohashi Y, Tachibana K, Kamiguchi K, Fujita H, Morimoto C. T cell receptor-mediated tyrosine phosphorylation of Cas-L, a 105-kDa Crk-associated substrate-related protein, and its association of Crk and C3G. *J Biol Chem* 1998; **273**(11)**:** 6446-51.

53. Katagiri K, Hattori M, Minato N, Irie S, Takatsu K, Kinashi T. Rap1 is a potent activation signal for leukocyte function-associated antigen 1 distinct from protein kinase C and phosphatidylinositol-3-OH kinase. *Mol Cell Biol* 2000; **20**(6)**:** 1956-69.

54. Xing L, Ge C, Zeltser R, Maskevitch G, Mayer BJ, Alexandropoulos K. c-Src signaling induced by the adapters Sin and Cas is mediated by Rap1 GTPase. *Mol Cell Biol* 2000; **20**(19)**:** 7363-77.

55. Sebzda E, Bracke M, Tugal T, Hogg N, Cantrell DA. Rap1A positively regulates T cells via integrin activation rather than inhibiting lymphocyte signaling. *Nat Immunol* 2002; **3**(3)**:** 251-8.

56. Ohba Y, Ikuta K, Ogura A, Matsuda J, Mochizuki N, Nagashima K *et al.* Requirement for C3G-dependent Rap1 activation for cell adhesion and embryogenesis. *Embo J* 2001; **20**(13)**:** 3333-41.

57. Ohashi Y, Iwata S, Kamiguchi K, Morimoto C. Tyrosine phosphorylation of Crk-associated substrate lymphocyte-type is a critical element in TCR- and beta 1 integrin-induced T lymphocyte migration. *J Immunol* 1999; **163**(7)**:** 3727-34.

58. Dustin ML, Starr T, Varma R, Thomas VK. Supported planar bilayers for study of the immunological synapse. *Curr Protoc Immunol* 2007; **Chapter 18:** Unit 18 13.

59. Dustin ML, Springer TA. T-cell receptor cross-linking transiently stimulates adhesiveness through LFA-1. *Nature* 1989; **341**(6243)**:** 619-24.

60. Springer TA, Dustin ML. Integrin inside-out signaling and the immunological synapse. *Curr Opin Cell Biol* 2012; **24**(1)**:** 107-15.

61. Makgoba MW, Sanders ME, Ginther Luce GE, Dustin ML, Springer TA, Clark EA *et al.* ICAM-1 a ligand for LFA-1-dependent adhesion of B, T and myeloid cells. *Nature* 1988; **331**(6151)**:** 86-8.

62. Astrof NS, Salas A, Shimaoka M, Chen J, Springer TA. Importance of force linkage in mechanochemistry of adhesion receptors. *Biochemistry* 2006; **45**(50)**:** 15020-8.

63. Mor A, Dustin ML, Philips MR. Small GTPases and LFA-1 reciprocally modulate adhesion and signaling. *Immunol Rev* 2007; **218:** 114-25.

64. Dustin ML, Bivona TG, Philips MR. Membranes as messengers in T cell adhesion signaling. *Nat Immunol* 2004; **5**(4)**:** 363-72.

65. Padrick SB, Rosen MK. Physical mechanisms of signal integration by WASP family proteins. *Annu Rev Biochem* 2010; **79:** 707-35.

66. Smith BA, Daugherty-Clarke K, Goode BL, Gelles J. Pathway of actin filament branch formation by Arp2/3 complex revealed by single-molecule imaging. *Proc Natl Acad Sci U S A* 2013; **110**(4)**:** 1285-90.

67. Sasahara Y, Rachid R, Byrne MJ, de la Fuente MA, Abraham RT, Ramesh N *et al.* Mechanism of recruitment of WASP to the immunological synapse and of its activation following TCR ligation. *Mol Cell* 2002; **10**(6)**:** 1269-81.

68. Barda-Saad M, Braiman A, Titerence R, Bunnell SC, Barr VA, Samelson LE. Dynamic molecular interactions linking the T cell antigen receptor to the actin cytoskeleton. *Nat Immunol* 2005; **6**(1)**:** 80-9.

69. Badour K, McGavin MK, Zhang J, Freeman S, Vieira C, Filipp D *et al.* Interaction of the Wiskott-Aldrich syndrome protein with sorting nexin 9 is required for CD28 endocytosis and cosignaling in T cells. *Proc Natl Acad Sci U S A* 2007; **104**(5)**:** 1593-8.

70. Snapper SB, Rosen FS, Mizoguchi E, Cohen P, Khan W, Liu CH *et al.* Wiskott-Aldrich syndrome protein-deficient mice reveal a role for WASP in T but not B cell activation. *Immunity* 1998; **9**(1)**:** 81-91.

71. Cannon JL, Burkhardt JK. Differential roles for Wiskott-Aldrich syndrome protein in immune synapse formation and IL-2 production. *J Immunol* 2004; **173**(3)**:** 1658-62.

72. Sims TN, Soos TJ, Xenias HS, Dubin-Thaler B, Hofman JM, Waite JC *et al.* Opposing effects of PKCtheta and WASp on symmetry breaking and relocation of the immunological synapse. *Cell* 2007; **129**(4)**:** 773-85.

73. Hanke JH, Gardner JP, Dow RL, Changelian PS, Brissette WH, Weringer EJ *et al.* Discovery of a novel, potent, and Src family-selective tyrosine kinase inhibitor. Study of Lck- and FynT-dependent T cell activation. *J Biol Chem* 1996; **271**(2)**:** 695-701.

74. Evans R, Lellouch AC, Svensson L, McDowall A, Hogg N. The integrin LFA-1 signals through ZAP-70 to regulate expression of high-affinity LFA-1 on T lymphocytes. *Blood* 2011; **117**(12)**:** 3331-42.

75. Wang H, Kadlecek TA, Au-Yeung BB, Goodfellow HE, Hsu LY, Freedman TS *et al.* ZAP-70: an essential kinase in T-cell signaling. *Cold Spring Harb Perspect Biol* 2010; **2**(5)**:** a002279.

76. Goldberg DR, Butz T, Cardozo MG, Eckner RJ, Hammach A, Huang J *et al.* Optimization of 2-phenylaminoimidazo[4,5-h]isoquinolin-9-ones: orally active inhibitors of lck kinase. *J Med Chem* 2003; **46**(8)**:** 1337-49.

77. Kumari S, Vardhana S, Cammer M, Curado S, Santos L, Sheetz MP *et al.* T Lymphocyte Myosin IIA is Required for Maturation of the Immunological Synapse. *Frontiers in immunology* 2012; **3:** 230.

78. Ilani T, Vasiliver-Shamis G, Vardhana S, Bretscher A, Dustin ML. T cell antigen receptor signaling and immunological synapse stability require myosin IIA. *Nat Immunol* 2009; **10**(5)**:** 531-9.

79. Carrizosa E, Gomez TS, Labno CM, Klos Dehring DA, Liu X, Freedman BD *et al.* Hematopoietic lineage cell-specific protein 1 is recruited to the immunological synapse by IL-2-inducible T cell kinase and regulates phospholipase Cgamma1 Microcluster dynamics during T cell spreading. *J Immunol* 2009; **183**(11)**:** 7352-61.

80. Dustin ML. Hunter to gatherer and back: immunological synapses and kinapses as variations on the theme of amoeboid locomotion. *Annu Rev Cell Dev Biol* 2008; **24:** 577-96.

81. Scholer A, Hugues S, Boissonnas A, Fetler L, Amigorena S. Intercellular adhesion molecule-1-dependent stable interactions between T cells and dendritic cells determine CD8+ T cell memory. *Immunity* 2008; **28**(2)**:** 258-70.

82. Chang JT, Palanivel VR, Kinjyo I, Schambach F, Intlekofer AM, Banerjee A *et al.* Asymmetric T lymphocyte division in the initiation of adaptive immune responses. *Science* 2007; **315**(5819)**:** 1687-91.

83. Buchholz VR, Flossdorf M, Hensel I, Kretschmer L, Weissbrich B, Graf P *et al.* Disparate individual fates compose robust CD8+ T cell immunity. *Science* 2013; **340**(6132)**:** 630-5.

84. Henrickson SE, Mempel TR, Mazo IB, Liu B, Artyomov MN, Zheng H *et al.* T cell sensing of antigen dose governs interactive behavior with dendritic cells and sets a threshold for T cell activation. *Nat Immunol* 2008; **9**(3)**:** 282-91.

85. Menasche G, Kliche S, Chen EJ, Stradal TE, Schraven B, Koretzky G. RIAM links the ADAP/SKAP-55 signaling module to Rap1, facilitating T-cell-receptor-mediated integrin activation. *Mol Cell Biol* 2007; **27**(11)**:** 4070-81.

86. Katagiri K, Maeda A, Shimonaka M, Kinashi T. RAPL, a Rap1-binding molecule that mediates Rap1-induced adhesion through spatial regulation of LFA-1. *Nat Immunol* 2003; **4**(8)**:** 741-8.

87. Raab M, Wang H, Lu Y, Smith X, Wu Z, Strebhardt K *et al.* T cell receptor "inside-out" pathway via signaling module SKAP1-RapL regulates T cell motility and interactions in lymph nodes. *Immunity* 2010; **32**(4)**:** 541-56.

88. Zhang Y, Wang H. Integrin signalling and function in immune cells. *Immunology* 2012; **135**(4)**:** 268-75.

89. Beinke S, Phee H, Clingan JM, Schlessinger J, Matloubian M, Weiss A. Proline-rich tyrosine kinase-2 is critical for CD8 T-cell short-lived effector fate. *Proc Natl Acad Sci U S A* 2010; **107**(37)**:** 16234-9.

90. Tachibana K, Urano T, Fujita H, Ohashi Y, Kamiguchi K, Iwata S *et al.* Tyrosine phosphorylation of Crk-associated substrates by focal adhesion kinase. A putative mechanism for the integrin-mediated tyrosine phosphorylation of Crk-associated substrates. *J Biol Chem* 1997; **272**(46)**:** 29083-90.

91. Regelmann AG, Danzl NM, Wanjalla C, Alexandropoulos K. The hematopoietic isoform of Cas-Hef1-associated signal transducer regulates chemokine-induced inside-out signaling and T cell trafficking. *Immunity* 2006; **25**(6)**:** 907-18.

92. Alexandropoulos K, Regelmann AG. Regulation of T-lymphocyte physiology by the Chat-H/CasL adapter complex. *Immunol Rev* 2009; **232**(1)**:** 160-74.

93. Samelson LE. Signal transduction mediated by the T cell antigen receptor: the role of adapter proteins. *Annu Rev Immunol* 2002; **20:** 371-94.

94. Babich A, Li S, O'Connor RS, Milone MC, Freedman BD, Burkhardt JK. F-actin polymerization and retrograde flow drive sustained PLCgamma1 signaling during T cell activation. *J Cell Biol* 2012; **197**(6)**:** 775-87.

95. Kumari S, Depoil D, Martinelli R, Judokusumo E, Carmona G, Gertler FB *et al.* Actin foci facilitate activation of the phospholipase C-gamma in primary T lymphocytes via the WASP pathway. *Elife* 2015; **4**.

96. Au-Yeung BB, Levin SE, Zhang C, Hsu LY, Cheng DA, Killeen N *et al.* A genetically selective inhibitor demonstrates a function for the kinase Zap70 in regulatory T cells independent of its catalytic activity. *Nat Immunol* 2010; **11**(12)**:** 1085-92.

97. Nishihara H, Maeda M, Oda A, Tsuda M, Sawa H, Nagashima K *et al.* DOCK2 associates with CrkL and regulates Rac1 in human leukemia cell lines. *Blood* 2002; **100**(12)**:** 3968-74.

98. Sanui T, Inayoshi A, Noda M, Iwata E, Oike M, Sasazuki T *et al.* DOCK2 is essential for antigen-induced translocation of TCR and lipid rafts, but not PKC-theta and LFA-1, in T cells. *Immunity* 2003; **19**(1)**:** 119-29.

99. Le Floc'h A, Tanaka Y, Bantilan NS, Voisinne G, Altan-Bonnet G, Fukui Y *et al.* Annular PIP3 accumulation controls actin architecture and modulates cytotoxicity at the immunological synapse. *J Exp Med* 2013; **210**(12)**:** 2721-37.

100. Guy CS, Vignali KM, Temirov J, Bettini ML, Overacre AE, Smeltzer M *et al.* Distinct TCR signaling pathways drive proliferation and cytokine production in T cells. *Nat Immunol* 2013; **14**(3)**:** 262-70.

101. Beemiller P, Krummel MF. Mediation of T-cell activation by actin meshworks. *Cold Spring Harb Perspect Biol* 2010; **2**(9)**:** a002444.

102. Beemiller P, Jacobelli J, Krummel MF. Integration of the movement of signaling microclusters with cellular motility in immunological synapses. *Nat Immunol* 2012; **13**(8)**:** 787-95.

103. Dobereiner HG, Dubin-Thaler BJ, Hofman JM, Xenias HS, Sims TN, Giannone G *et al.* Lateral membrane waves constitute a universal dynamic pattern of motile cells. *Phys Rev Lett* 2006; **97**(3)**:** 038102.

104. Carrasco YR, Fleire SJ, Cameron T, Dustin ML, Batista FD. LFA-1/ICAM-1 interaction lowers the threshold of B cell activation by facilitating B cell adhesion and synapse formation. *Immunity* 2004; **20**(5)**:** 589-99.

105. Carpenter AE, Jones TR, Lamprecht MR, Clarke C, Kang IH, Friman O *et al.* CellProfiler: image analysis software for identifying and quantifying cell phenotypes. *Genome Biol* 2006; **7**(10)**:** R100.

FIGURE LEGENDS

FIGURE 1. TCR microcluster movement is impaired in the absence of Cas-L. (**A**) Western blot of total cell lysates from $CD8^+$ T cells isolated by negative selection from spleen of Cas-L-null ($Cas\text{-}L^{-/-}$) mice, and from the control Cas-L heterozygous littermates (WT). A monoclonal antibody for Cas-L was used to assess the presence of Cas-L. (**B**) Cells were fixed in 2% paraformaldehyde 15 min after seeding, and images of synapses formed in both cell types were acquired in both channels. Red = TCR; blue = ICAM-1; yellow = synapse outline. Scale bar = 2 μm. (**C**) Radial profiles of TCR and ICAM-1 fluorescence intensities at the synapses of WT and $Cas\text{-}L^{-/-}$ cells (radial sweep averaged from at least 50 cells in each cell type and two independent experiments). Solid and dashed lines represent WT and $Cas\text{-}L^{-/-}$ cells, respectively. Red = TCR, blue = ICAM-1. P-value < 0.05 (**D**) Time-lapse images of TCR microcluster formation and translocation at the immunological synapse. Yellow arrowheads highlight individual TCR microcluster position at the synapse at different time points. Freshly isolated T cells from WT or $Cas\text{-}L^{-/-}$ mice were seeded on a bilayer embedded with fluorescently-labeled antibody to TCR and ICAM-1, and imaged in a TIRF microscope to follow immunological synapse formation. Simultaneous imaging of four different fields of the bilayer was performed with a 100X objective, with an acquisition rate of 13s between frames. Scale bar = 5μm. (**E**) Average speed of translocation of individual TCR microclusters during synapse formation. Mean ± standard error of the mean represent two independent experiments. At least five individual microclusters per cell were analyzed in at least three cells. One asterisk indicates p-value ≤ 0.05. (**F**) Change in mean fluorescence intensity of TCR microclusters during synapse formation in WT and $Cas\text{-}L^{-/-}$ cells. Mean values of four cells of each type, pooled from two independent experiments. P-value < 0.0005 (**G**) Change in area occupied by TCR microclusters at the synapse of WT and $Cas\text{-}L^{-/-}$

cells analyzed in D (mean values of four cells of each type, pooled from two independent experiments).

FIGURE 2. Phosphorylated Cas-L co-localizes with new TCR microclusters at the periphery of the immunological synapse. (**A**) TIRF images of synapses from mouse spleen $CD8^+$ T cells fixed at two minutes after seeding on bilayers embedded with fluorescently-labeled antibody to TCR (red) and ICAM-1 (blue), and stained with an antibody specific for phospho-tyrosine repeats in the substrate domain of Cas-L (pCasL, green). Yellow boxes are expanded on the right panel. Arrowheads highlight co-localization of TCR microclusters and phospho-Cas-L. Scale bar = 2μm. (**B**) Cas-L phosphorylation at the synapse depends on Src-family kinase activity. Scale bar = 2μm. (**C**) Cas-L recruitment to TCR microclusters depends on Src-family kinases activity. Dot plots display the median (central line), ± 1.5 x interquartile range (whiskers). One asterisk represents p-value ≤ 0.05; two asterisks represent p-value ≤ 0.005; three asterisks mean p-value ≤ 0.0005; data represents at least 30 cells from two independent experiments. Graphs display 30 cells from two experiments pooled in one graph. (**D-E**) Cas-L phosphorylation at the immunological synapse is significantly decreased after inhibition of Lck by treatment with piceatannol or an Lck selective inhibitor. Mean values ± standard error of the mean are representative of at least 30 cells (for each condition) from two independent experiments. Scale bar = 2μm. One asterisk indicates p-value ≤ 0.05; three asterisks p-value ≤ 0.0005.

FIGURE 3. Cas-L$^{-/-}$ T cells show impaired release of Ca^{2+} from intracellular stores. (**A**) Time-lapse images of T cells from WT or Cas-L$^{-/-}$ mice pre-incubated with Calcium ion fluorescent dye Fluo4, and seeded on glass coverslips coated with antibodies against TCR/CD28 and ICAM-1. Changes in free intracellular Ca^{2+} levels were captured in the 488nm channel (widefield, Fluo4 top panel), and images of the contact between a cell and the coverslip were visible through internal reflection microscopy (IRM bottom panel). Ionomycin was added to the medium at approximately 20 min (+Iono), and EGTA was added at approximately 30 min. The acquisition rate was 4s between frames. Scale bar = 5μm. (**B**) Changes in Ca^{2+} levels were plotted across time for at least ten individual cells of each cell type from two independent experiments. Fluorescence intensity values were normalized for each individual cell by dividing background-corrected intensity values by the absolute maximum intensity value measured after adding ionomycin (imax2). (**C**) Levels of free intracellular Ca^{2+} in Cas-L$^{-/-}$ cells only rise up to 47%±9% of their maximum potential (as measured by imax2), while in control WT cells Ca^{2+} levels peak at 87%±11% of their maximal potential (p-value ≤ 0.005). (**D**) No significant change in the levels of sustained free intracellular Ca^{2+} (sustained/imax2) between Cas-L$^{-/-}$ and control WT cells ("n.s.": non-significant; error bars represent standard error of the mean from two independent experiments). (**E**) PLCγ1 phosphorylation (pPLCγ1, green) is reduced at the synapse of Cas-L$^{-/-}$ T cells. Scale bar = 5μm. (**F**) Co-localization of phospho-PLCγ1 with TCR microclusters is impaired in Cas-L$^{-/-}$ cells. Dot plots display the median (central line) ± 1.5 x interquartile range (whiskers). One asterisk means p-value ≤ 0.05, three asterisks mean p-value ≤ 0.0005; data represents at least 30 cells from two independent experiments.

FIGURE 4. Cas-L$^{-/-}$ T cells exhibit impaired adhesion and erratic migration. (**A**) TIRF microscopy images show the central TCR clusters (left panel) and cell bilayer contact area (right panel) at 15min after seeding. Stable synapses are marked with a yellow asterisk, and the colored lines represent the tracks of migrating cells. Scale bars = 10μm. (**B**) Cas-L$^{-/-}$ cells form significantly less stable synapses than WT cells (p-value ≤ 0.0005). Values of averages ± standard error of the mean are representative of at least 30 cells of each type and three independent experiments. (**C**) Quantification of adhesion and migration parameters of WT and Cas-L$^{-/-}$ cells (values represent mean ± standard error of the mean of at least 30 cells from three independent experiments). (**D-E**) Cas-L$^{-/-}$ cells exhibit deficient spreading, having smaller contact areas, and more circular contact areas, in comparison to control cells. (**F**) ICAM-1 recruitment to the synapse is impaired in Cas-L$^{-/-}$ cells, especially at early time points of synapse formation. (**G**) Providing bilayers with increasing amounts of ICAM-1 is not sufficient to rescue synapse instability exhibited by Cas-L$^{-/-}$ cells. One asterisk: p-value ≤ 0.05; "n.s.": non-significant; data represents three independent experiments.

FIGURE 5. Cas-L phosphorylation is dependent on actin polymerization. (**A**) Actin disruption affects the radial profiles of phospho-Cas-L (pCasL) intensity at the synapse. T cells treated for 30min with DMSO, or 60nM and 200nM Cytochalasin D (CytoD) were seeded on anti-CD3ε/ICAM1-embedded bilayers, allowed to interact with the bilayers for 2min, fixed with 2% paraformaldehyde, and stained with an antibody specific for phosphotyrosine residue repeats in the substrate domain of Cas-L. The synapses were imaged with TIRFM, the levels of mean fluorescence intensity of pCas-L were measured, processed, and the average radial profiles and standard error of the mean of at least 30 cells per condition were plotted (data represents two independent experiments). (**B**) Confocal slices from the synapses of WT and Cas-L$^{-/-}$ cells, and corresponding vertical section profiles. The border between lamella and lamellipodia structures is lost in synapses of Cas-L$^{-/-}$ cells. Scale bars = 2μm. (**C**) Radial profiles of f-actin in synapses of WT and Cas-L$^{-/-}$ T cells indicated lower f-actin accumulation at the synapses of Cas-L$^{-/-}$ T cells. Cells were seeded on bilayers, fixed at 2min, and stained with fluorescently-labeled phalloidin (green). Curves represent the mean ± standard error of the mean of at least 30 cells from three independent experiments. (**D**) Phospho-Cas-L levels at the synapse are dependent on Arp2/3 activity. T cells were treated with a small molecular inhibitor of Arp2/3 (CK666), or DMSO as control. Three asterisks: p-value ≤ 0.0005. (**E**) Phospho-Cas-L levels at the synapse are dependent on WASp activity. WASp$^{-/-}$ T cells or WT cells were seeded on bilayers, fixed at 2min, and stained for phospho-Cas-L. (**F**) Cas-L and PKCθ play opposing roles in regulating synapse stability. T cells from Cas-L$^{-/-}$ mice were seeded on bilayers, and 20min after seeding a small molecule inhibitor for PKCθ (C20) was added to the medium (at 10μM or 33μM) and its effect was followed for another 20min. Graph reflects the change in the number of new synapses

formed after C20 treatment relative to the DMSO control. Values represent mean ± standard error of the mean of at least 30 cells from 3 independent experiments.

FIGURE 6. Working model illustrating the critical steps that lead to cytoskeletal stretch-dependent Cas-L activation and TCR signaling. Based on our observations, we propose a model where the initial steps of TCR ligation and clustering (1-2), assembly of actin nucleating factors (3) and initial f-actin polymerization at TCR microclusters (4) take place independently of Cas-L, and the subsequent steps leading to integrin activation and stabilization of lamellipodia structures (6), and TCR transport (7), are regulated by actin-dependent Cas-L activation at TCR microclusters. In turn, this mechanical activation of Cas-L acts via a potential feedback loop that leads to TCR signal amplification (8-9) thus stabilizing the immunological synapse.

MOVIE LEGENDS

Movie 1: Impaired TCR cluster movement at the immunological synapse of Cas-$L^{-/-}$ T cells. Time-lapse imaging series of TCR microclusters forming at the immunological synapse. Freshly isolated T cells from control (top panel) or Cas-$L^{-/-}$ (bottom panel) mice were seeded on bilayers embedded with fluorescently-labeled antibody to TCR and ICAM-1, and imaged in a TIRF microscope to follow immunological synapse formation. In control T cells (top panel), TCR microclusters assembled at the periphery of the synapse within seconds of interaction with the bilayer and moved rapidly towards the center, accumulating in one sharply defined bright spot in the center of the synapse. In contrast, in Cas-$L^{-/-}$ T cells (bottom panel), movement and accumulation of TCR microclusters at the synapse was impaired. The acquisition rate was 13s between frames (movie duration: approximately 3 minutes). Scale bar = 5μm.

Movie 2: Cas-$L^{-/-}$ T cells show impaired release of Ca^{2+} from intracellular stores. Time-lapse imaging of T cells from control (top panel) or Cas-$L^{-/-}$ (bottom panel) mice pre-incubated with Calcium ion (Ca^{2+}) fluorescent dye Fluo4, and seeded on glass coverslips coated with antibodies against TCR/CD28 and ICAM-1. Changes in free intracellular Ca^{2+} levels were captured in the 488nm channel (widefield, Fluo4), and images of the cell-coverslip contact area were visible through internal reflection microscopy (IRM). When T cells touched the antibody-coated coverslip they exhibited a sharp increase of Fluo-4 fluorescence intensity corresponding to Ca^{2+} released from intracellular stores, followed by a decrease of fluorescence intensity down to baseline level. Cas-$L^{-/-}$ T cells exhibited a lower value of first Ca^{2+} peak than control cells. In this

movie, ionomycin, an ionophore that transports Ca^{2+} across membranes bypassing a TCR-mediated signal, was added to the medium at approximately 10 min, and it induced an absolute maximum Fluo-4 intensity peak in both cell types. Then, EGTA was added to the medium at approximately 20 min and the Fluo-4 intensity returned to minimum levels. The acquisition rate was 4s between frames (movie duration approximately 25 minutes). Scale bar = 10μm.

Movie 3: Cas-$L^{-/-}$ T cells form unstable immunological synapses. TIRF microscopy time-lapse imaging of control (top panel) and Cas-$L^{-/-}$ (bottom panel) T cells seeded on bilayers with anti-CD3ε and ICAM-1 shows the accumulation of TCR clusters at the center of the synapse (on the left) and cell bilayer contact area (on the right). The majority of Cas-$L^{-/-}$ T cells (bottom panel) failed to form a stable synapse, quickly polarized after contacting the bilayers, and migrated erratically. In contrast, the majority of control T cells (top panel) formed persistent stable synapses that remained in the same initial position during the course of the experiment, while a small fraction of the population polarized and exhibited directed migration. The acquisition rate was 30s between frames (movie duration approximately 9 minutes). Scale bar = 10μm.

SUPPLEMENTARY FIGURE 1 LEGEND

Supplementary Figure 1: (A-B) Levels of ZAP70 and phosphorylated ZAP70-Y319 are unchanged in Cas-L$^{-/-}$ T cells. Western blot analyses of total lysates from wild type and Cas-L$^{-/-}$ T cells. (C) Cas-L is not required for TCR-mediated IL-2 production. Supernatant from wild type mouse splenic CD8^{+} T cells incubated for 48h on anti-CD3ε/ICAM-1 coated chambers (both at 5 μg/ml) was analyzed by ELISA for levels of secreted IL-2 (see Materials and Methods). (D-E) Cas-L deficiency has no effect on the expression levels of LFA-1 on naïve and activated CD8^{+} T cells from the peripheral blood of mice 8 days after infection with listeria monocytogenes (5000 cfu) expressing chicken ovalbumin (Lm-Ova). At 8 days following infection, peripheral blood was analyzed for the presence of Ova-specific CD8^{+} T cells via flow cytometry. Naïve cells were identified as CD8^{+}LFA1^{low}. Activated cells were identified as CD8^{+}LFA1^{high}. Mean fluorescence intensity of LFA1 from the corresponding populations is plotted as the mean ± standard deviation of the mean of 4 mice per group. (F) Inhibition of src-family kinases leads to increased co-localization of phospho-Cas-L with the TCR. Pearson's correlation coefficient was computed to analyze the effect of PP2 treatment on the co-localization between phospho-Cas-L and TCR. This analysis compares the overlap between phospho-Cas-L and TCR across the entire synapse area (whole synapse) or only at TCR clusters. After treating cells with PP2 (10 μM), the signal of phospho-Cas-L was more strongly co-localized with TCR clusters than in the absence of PP2 (i.e. DMSO control). Dot plots display the median (central line) ± 1.5 x interquartile range (whiskers), three asterisks p-value ≤ 0.0005. Data represents at least 30 cells from two independent experiments.

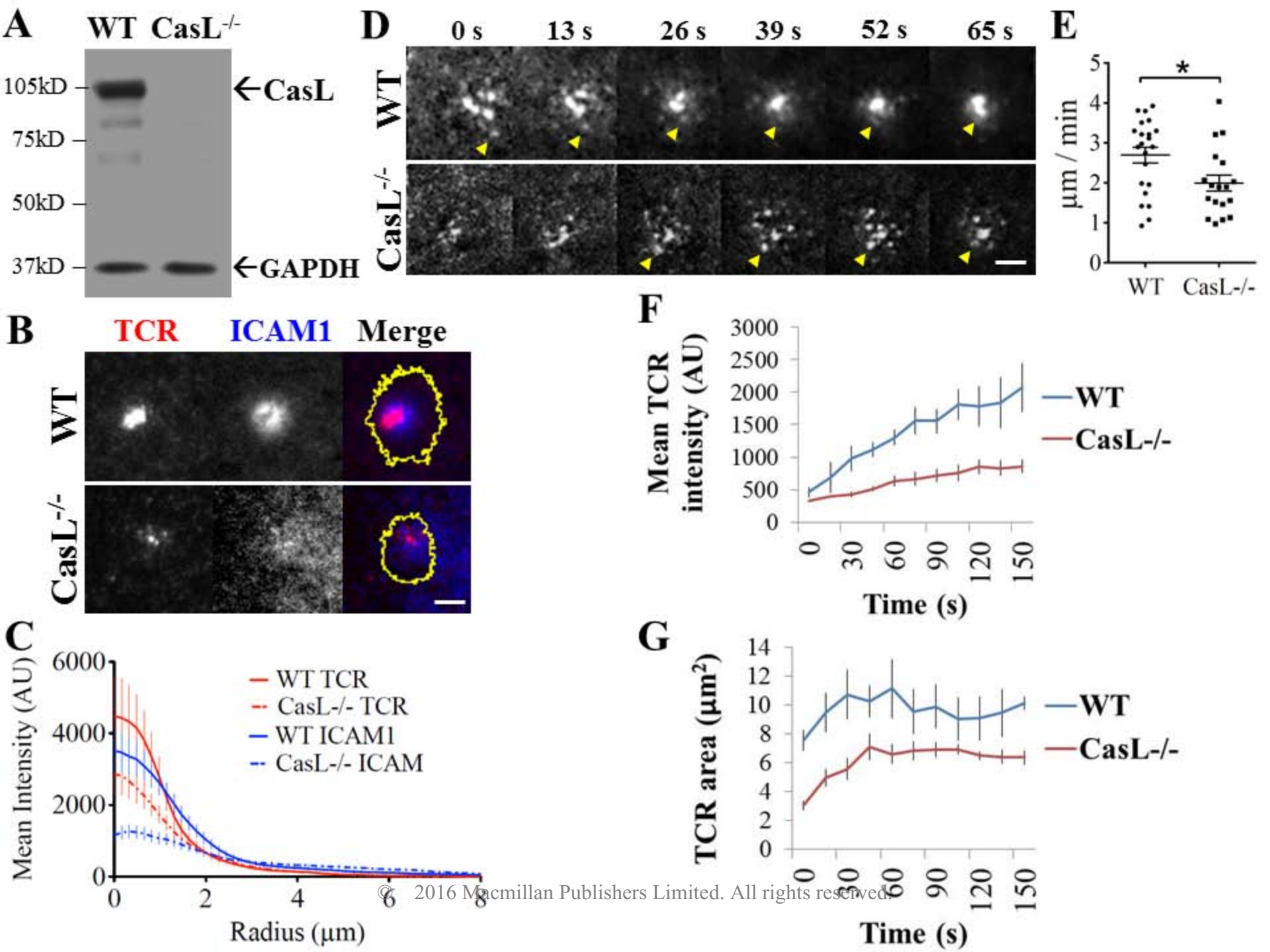

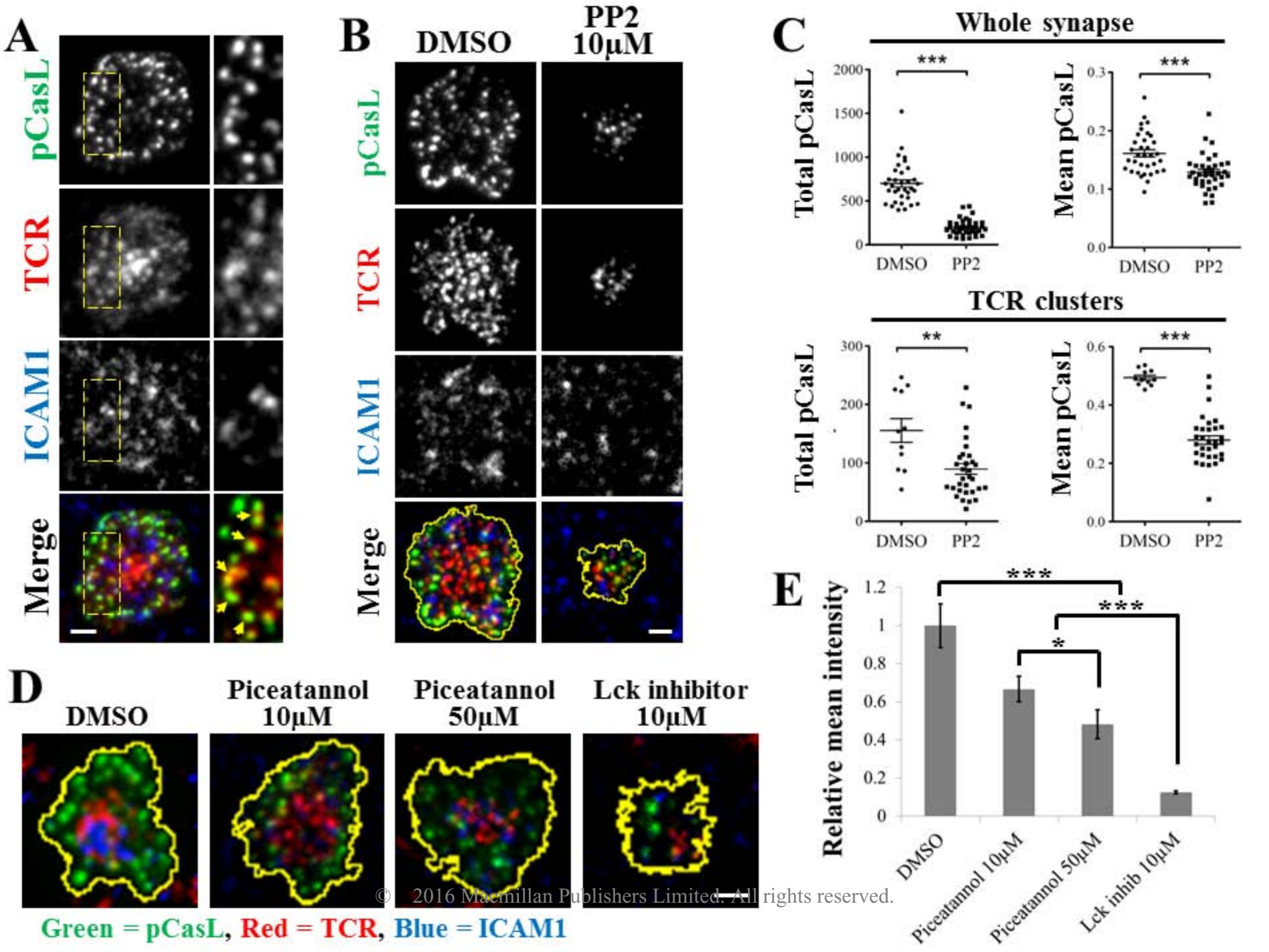

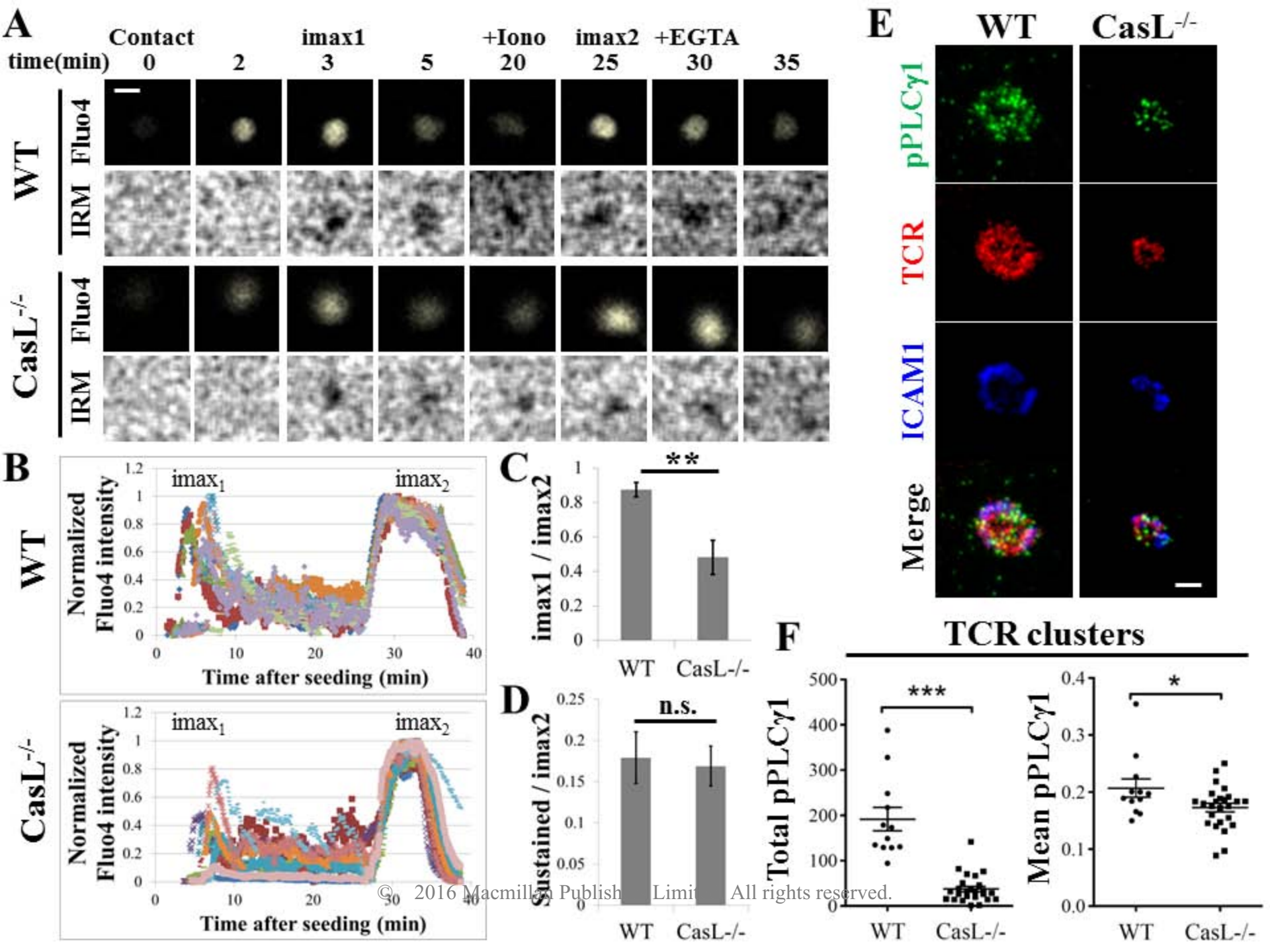

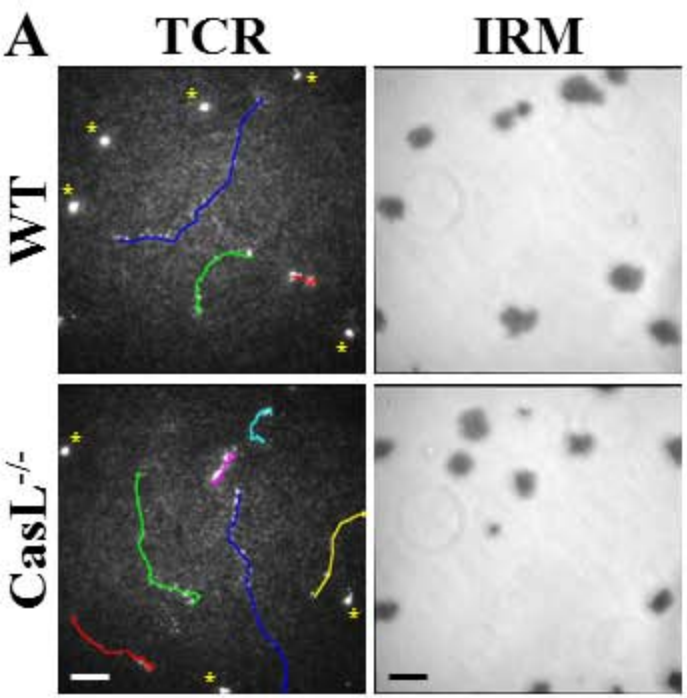

C

@ t = 15 min	Synapse area (μm²)	Stable synapses (%)	Migrating cells (%)	Migration speed (μm min⁻¹)	Distance travelled (μm)
WT	44.5 ± 7.7	71 ± 4	29 ± 4	5.3 ± 0.91	48 ± 6.0
CasL-/-	20.1 ± 2.3	37 ± 8	63 ± 8	3.5 ± 0.51	28 ± 1.3